

1 We would like to thank both reviewers for the positive and constructive comments. Their  
2 suggestions have helped improve our study. Our responses are listed below in blue and italic.

3 Response to reviewer 1

4 Overall Review

5 The article presents a detailed exercise of upscaling photosynthesis from the leaf scale to the  
6 stand level for the climatic conditions and vegetation distribution corresponding to the  
7 EucFACE experiment (forest stand dominated by *Eucalyptus tereticornis*) and thus it includes  
8 ambient and elevated CO<sub>2</sub> (eCO<sub>2</sub>) scenarios. Upscaling leaf-level response to tree and forest  
9 stand scale is a long-standing problem in biogeoscience and while it has been tackled in  
10 various ways in the literature, the study presented here is innovative for the thoroughness and  
11 level of detail included in the analysis. Furthermore, the analysis is carried out for ambient  
12 and eCO<sub>2</sub> conditions using a terrestrial biosphere model (MAESPA) that represents explicitly  
13 each tree and solve the canopy using multiple layers and accounts in each layer for multiple  
14 points representing radial variability in incoming light. The study also accounts for the  
15 acclimation response of photosynthesis and it is strongly constrained by observations, which  
16 is rarely the case in other similar studies. The study convincingly shows that a strong increase  
17 in leaflevel light-saturated photosynthesis (+33%) under eCO<sub>2</sub> reflects in a minor increase in  
18 stand level GPP (10%) because of the prevalence of electron transport limitations in  
19 photosynthesis and to a minor extent downregulation of photosynthetic capacity due to the  
20 leaf acclimation to eCO<sub>2</sub>. Results also show a large uncertainty in computing GPP at the  
21 stand level when a small area (corresponding to a CO<sub>2</sub> enrichment ring) is considered. While  
22 upscaling photosynthesis at the forest stand scale is not a new task, the way this problem is  
23 solved here, represents a scientific advancement because it is presented in the context of a  
24 FACE experiment and provide a number of interesting discussion points on mechanistic  
25 model parameterization and uncertainties (e.g., the role of the curvature for electron transport,  
26 the  $J_{c,max}/V_{c,max}$  ratio, photosynthesis acclimation, forest stand heterogeneity). It is clearly  
27 shown that translating leaf-level responses of CO<sub>2</sub> effects to the ecosystem scale is very  
28 misleading and most important the study provides mechanistic explanations for the  
29 differences. The search for the reasons and the clear explanations provided concerning  
30 subcomponents of the photosynthesis model (e.g., Rubisco vs. electron transport limited, or  
31 acclimation of photosynthetic capacity) represents an innovative approach, which I did not  
32 see before in the literature. For these reasons, beyond the importance of estimating GPP in  
33 ambient and eCO<sub>2</sub> conditions that will serve future studies in the context of the EucFACE  
34 experiment, the article represents an important piece of work for the mechanistic  
35 understanding of ecosystem responses to elevated CO<sub>2</sub>.

36 The article is overall very well written and presented. In summary, I think the manuscript is  
37 making an important contribution to the field and I sincerely congratulate the authors for this  
38 nice piece of work. In the following, I just have a number of minor comments that can be  
39 helpful to improve further the presentation of this work.

40 Sincerely,

41 Simone Fatichi

42 *Response: We would like to thank the reviewer for his detailed and positive evaluation of our*  
43 *work. We have modified the manuscript according to his comments.*

44

45 Minor comments

46 P.2 Line 34-37. The difference between canopy scale “direct response” of +11% and  
47 the mean actual response of 6%, while very clear in the manuscript, it is not so clear at  
48 the abstract level. Maybe introducing the concept of “uncertainty” associated with the  
49 variability across rings or something associated to the “actual field response” according  
50 to the experimental configuration may help.

51 *Response: We have changed the text to read:*

52 *‘After taking in account the baseline variability in leaf area index across plots, we estimated a field GPP*  
53 *response to  $eC_a$  of 6% with a 95% confidence interval (-2, 14%).’*

54

55 P.3 Line 51. The “hence” here is out of place, because the causality is not straightforward. An  
56 increase in carbon uptake does not necessarily lead to an increase in the amount of carbon  
57 stored in the ecosystem. The authors are well aware of this. Something like “which in turn  
58 could potentially increase. . .” will be more correct.

59 *Response: We have changed this line to read:*

60 *“These physiological responses at the leaf scale can increase ecosystem carbon uptake, which in*  
61 *turn may result in increased carbon storage in the ecosystem, mitigating against the rise in  $C_a$ .”*

62

63 P.3. Line 57. A short overview of main disagreements between various studies is  
64 provided in Fatichi et al. 2019.

65 *Response: We thank the reviewer for bringing the paper to our attention. The citation is now*  
66 *added to the paper.*

67

68 P.3. Line 57-68. I think this paragraph would benefit from referring to the estimates  
69 of global terrestrial C sink. While the attribution of the land C-sink is still debated, an  
70 average C-sink of 20–30 g C year<sup>-1</sup> m<sup>-2</sup> over vegetated land in the last decades is not

71 a detail in the overall story about eCO<sub>2</sub>.

72 *Response: We have referred to the land carbon sink in the text:*

73 *'Similarly, the global carbon budget indicates a strong sink for carbon on land (Le Quéré et al.,*  
74 *2018).'*

75

76

77 P. 4. Line 80. While, practically, I would agree in defining the response of GPP to eCO<sub>2</sub>

78 an upper bound. Theoretically, this is not a limit, if for some reason, plants in eCO<sub>2</sub>

79 conditions will be able to do maintenance with half of the respiration costs, then the

80 NPP response could be larger than the GPP response. I think a “reference value” is

81 more correct than an “upper-bound”.

82 *Response: We have modified the line to read:*

83 *“The response of GPP is important because it provides a reference point against which to*  
84 *compare the response of other components of ecosystem carbon balance, such as above-*  
85 *ground growth.”*

86

87 P.4. Line 115 and P.6 Line 161 and 166. Yang et al. 2019 is missing from the reference

88 list, overall, I would avoid referring to papers, which are not published.

89 *Response: The paper is now accepted at Tree Physiology*

90 *(<https://doi.org/10.1093/treephys/tpz103>). We have added the reference to the list.*

91

92 P.4 Line 116 and P.6 Line 170-171. I would not mix the “meteorological forcing” with the

93 “model parameterization”. The two aspects are different from a modeling perspective, one

94 represents the inputs to the model, the other (e.g., physiological and structural attributes)

95 represents model parameters, or prognostic variables if these are time dynamics and

96 computed in the model. One can use the same model parameterization with different

97 meteorological inputs and the other way around.

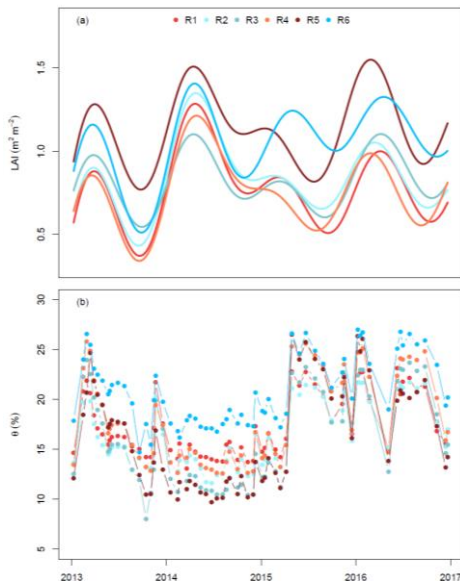
98 *We agree with the reviewer and deleted ‘meteorological’ in the sentence.*

99

100 P.6 L.173. Figure 2b. I am strongly encouraging to avoid using a linear interpolation

101 for soil moisture values at least in its graphical representation. Soil moisture temporal  
102 dynamics have a fast and strong response to rainfall events. Linearly interpolating  
103 biweekly value is creating a misleading perception of the real temporal dynamics of  
104 soil moisture. I would prefer to have just the points when the soil moisture values have  
105 been collected rather than the current representation where raising and descending  
106 soil moisture dynamics are often unrealistic.

107 *Response: We have adapted the suggestion by plotting the soil wwater content as dots and*  
108 *revised the figure legend. Thank you for this suggestion. We experimented with removing the*  
109 *lines from this plot as suggested but it is hard to see anything without the lines.*



110

111

112

113 P.7. Line 220. Just a suggestion. Maybe the Fig. S1 could be included in the main  
114 manuscript.

115 *Response: We are glad to see that the reviewer likes fig s1. The fig works well as a*  
116 *conceptual figure showing how the model works but does not related directly to the inputs*  
117 *and results of the model. We thus decide to leave it in the supplementary material.*

118

119 P.9 Line Table 1. I know that in literature it is quite typical to report  $\mu\text{mol}$  only. However,  
 120 this is not very precise, especially when we are dealing with photosynthesis. I would  
 121 suggest to explicitly say  $\mu\text{mol}$  of what, e.g.,  $\mu\text{mol-CO}_2$ ,  $\mu\text{mol-H}_2\text{O}$ ,  $\mu\text{mol-electrons}$  or  
 122 better  $\mu\text{mol-Eq.}$  as in the original Farquhar et al. 1980.

123 *We have revised the table as suggested:*

124 *Table 1. Summary table of parameter definitions, units, and sources used in this study.*

Parameters	Definitions	Units	Values	Eqn.
$\alpha_j$	Quantum yield of electron transport rate	$\mu\text{mol electron } \mu\text{mol}^{-1}$ photon	0.30	S7
$a$	Fitted slope of LA and DBH	$\text{m}^2 \text{m}^{-1}$	492.6	4
$a_{\text{abs}}$	Absorptance of PAR	fraction	0.825	S4
$b$	Fitted index of LA and DBH	-	1.8	4
$c_D$	Slope of $V_{\text{cmax}}$ to $D$	$\text{kPa}^{-1}$	0.14	3
$\Delta S$	Entropy factor	$\text{J mol}^{-1} \text{K}^{-1}$	639.60 ( $V_{\text{cmax}}$ ); 638.06 ( $J_{\text{max}}$ )	S5
$E_a$	Activation energy	$\text{J mol}^{-1}$	66386 ( $V_{\text{cmax}}$ ); 32292 ( $J_{\text{max}}$ )	S5
$g_{1,\text{max}}$	Maximum $g_1$ value	$\text{kPa}^{0.5}$	5.0	2
$H_d$	Deactivation energy	$\text{J mol}^{-1}$	200000	S5
$\theta_j$	Convexity of electron transport rate to $Q_{\text{APAR}}$	-	0.48	S8
$\theta_{\text{max}}$	Upper limit of soil water content above which $g_1$ is maximum	-	0.240	2
$\theta_{\text{min}}$	Lower limit of soil water content below which $g_1$ is zero	-	0.106	2
$J_{\text{max},25}$	Value of $J_{\text{max}}$ at 25°C	$\mu\text{mol electron m}^{-2} \text{s}^{-1}$	159	3
$k_T$	Sensitivity of $R_{\text{dark}}$ to temperature	$^{\circ}\text{C}^{-1}$	0.078	S6
$q$	The non-linearity of the $g_1$ dependence of $\theta$	-	0.425	2
$R_{\text{day},25}$	Light respiration rate	$\mu\text{mol C m}^{-2} \text{s}^{-1}$	0.9	S6
$R_{\text{dark},25}$	Dark respiration rate	$\mu\text{mol C m}^{-2} \text{s}^{-1}$	1.3	S6
$R_{\text{gas}}$	Gas constant	$\text{J mol}^{-1} \text{K}^{-1}$	8.314	S5
$V_{\text{cmax},25}$	Value of $V_{\text{cmax}}$ at 25°C	$\mu\text{mol C m}^{-2} \text{s}^{-1}$	91 (ambient); 83 (elevated)	3

125

126

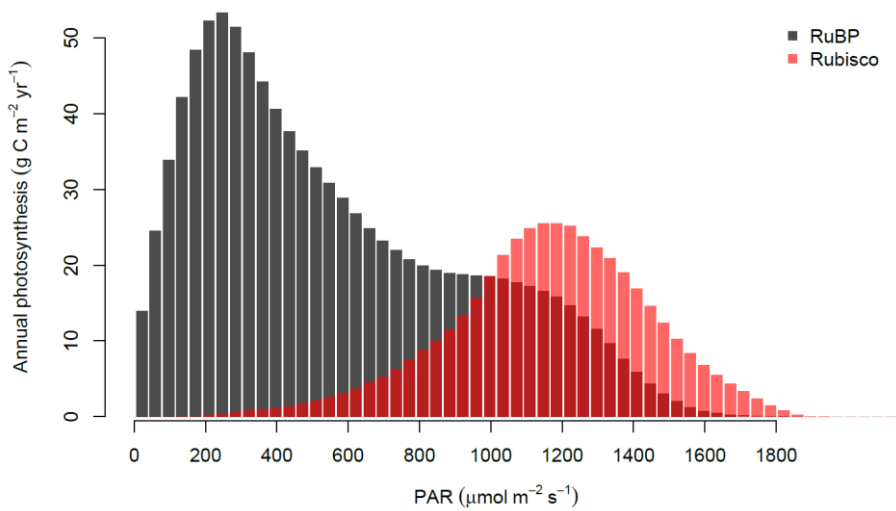
127 P.10. Line 286-290. Did you check if with MAESPA you get the same +33% of leaflevel  
 128 photosynthesis if you simulated the same environmental conditions of the 600 A-Ci curves?  
 129 Very likely, yes, because these are used to estimate the photosynthesis parameters, but just as  
 130 a double check.

131 *Response: The leaf gas exchange model in MAESPA is the same leaf-scale model as the*  
 132 *'photosyn' function implemented in the 'plantecophys' R package. We did not check the full*  
 133 *MAESPA model but checked the leaf gas exchange model in the R package, which can*  
 134 *reproduce the 33% value depending on parameterisation.*

135

136 P.10 Figure 6 and 7. In Fig.7 is reported incident PAR and in Fig. 6 absorbed PAR, even  
137 though one refer to the stand scale and the other to the leaf-level, I think it would have  
138 been better to use either absorbed or incident PAR in both of them for comparison.

139 *Response: We have changed Fig 6 to PAR so that both figures are directly comparable.*



140

141

142 P. 11. Line 318. From the Supp. Material, the curvature for electron transport  $\theta_j$  is  
143 also used as curvature and for overall photosynthesis (Eq. S8). These two values are  
144 typically different in models (e.g., Bonan et al 2011). This needs to be specified in the  
145 manuscript as well. The reference  $\theta_j = 0.85$  is typically assumed for the curvature and  
146 for the overall photosynthesis, rather than for the curvature of electron transport, which  
147 is typically lower in some models (0.7, Bonan et al 2011, Fatichi et al 2016). This needs  
148 to be discussed.

149 *Response: We have modified L320-321 to read:*

150 *“We explored this effect by investigating the effect of varying the convexity,  $\theta_j$ , which is assumed to be the same*  
151 *as the convexity of overall photosynthesis.”*

152 and L422-423 to read:

153 “The parameter value we fitted to data measured in situ ( $\theta_J = 0.48$ ) is lower than the value commonly assumed  
154 in the models (e.g., 0.7 in Bonan et al., 2011). Note that some model studies assume that  $\theta_J$  to be lower than the  
155 convexity of overall photosynthesis (typically over 0.8; e.g., 0.9 in Medlyn et al., 2002; 0.85 in Haverd et al.,  
156 2018). Here we assumed that the convexity of electron transport rate and overall photosynthesis are the same  
157 (see Supplementary Text S1 for details).”

158 We added justifications in Supplementary Text S1:

159 ‘The assumptions of the quantum yield and convexity being the same between  $J$  and overall photosynthesis are  
160 further explored by comparing the photosynthesis predicted by ‘photosyn’ function with the fitted  $\alpha_A$ , and  $\theta_J$  to  
161 the measured light response curve. There’s good agreement with a root mean square error of  $2.3 \mu\text{mol m}^{-2} \text{s}^{-1}$   
162 and a  $R^2$  of 0.92, suggesting the assumptions are appropriate in our site. ’

163

164 P. 12. Line 377. I am honestly impressed by the inter-ring differences in GPP. I think  
165 these are mostly related to the relative small size of the rings. Or better, the size  
166 is quite large in comparison to experimental capabilities but relative small to average  
167 forest stand heterogeneities.

168 *Response: Despite the relatively consistent overstorey vegetation, this mature forest has*  
169 *remained unmanaged for at least over 90 years, subject to native and variable environmental*  
170 *fluctuations. We therefore believe that spatial heterogeneity is the major driver of the inter-*  
171 *ring variability in GPP.*

172

173 P.12 Line 388. Renchon et al 2018 is not in the reference list.

174 *Response: We have added the paper to the reference list.*

175

176 Eq (S3) The denominator should be  $C_i + 2\Gamma$  rather than  $C_i + \Gamma$  (e.g., Wang and Leuning,  
177 1998, Dai et. 2004, Bonan et al 2011);

178 *Response: Thanks, the equation has been corrected.*

179

180

181 **Response to reviewer 2**

182 This manuscript synthesizes a large amount of data from the EucFACE project to examine  
183 the effects of Rubisco- versus RuBP limitation on photosynthesis under elevated  
184 CO<sub>2</sub>. The authors present leaf-level measurements, leaf-level modeling, and canopy  
185 scale modeling of ambient versus elevated CO<sub>2</sub> conditions to illustrate that current  
186 projections of GPP under elevated CO<sub>2</sub> are overestimated in mature forests due to biases  
187 towards light-saturated leaves. This work is scientifically relevant and pedantic. I want  
188 to commend the authors on their efforts and have minor suggestions to improve the  
189 presentation and make the work clearer to a wider audience.

190  
191 The introduction is extremely well written and provides appropriate context for the work  
192 being conducted within the manuscript. The methodology is thoughtfully presented,  
193 and justification was given for parameter choices in the model. The amount of data  
194 used to represent the system is commendable and I appreciate the attention to detail.  
195 I find the presentation of soil moisture to be the weakest element of the methodology  
196 and would recommend a little more attention paid to it as it is one of the few varying  
197 parameters between the replicates. The presentation of the results would be strengthened  
198 by more clearly delineating measurements vs. leaf scale modeling vs. canopy scale modeling.  
199 I would personally be very interested in seeing some of the rawer data forms (e.g., timeseries  
200 of canopy model) in addition to the synthesized percent changes. While this may be a  
201 question of style, I found the figure captions to contain relevant information that was missing  
202 from the text. I would include more of that information in the text for clarity. Figures are  
203 adequate, but the figure legends are not descriptive (esp. Fig 2 and 4-7) and the long captions  
204 make it difficult to distinguish between the different replicates, responses, etc.

205  
206 Overall well done and I'm excited to see this work published!

207  
208 *Response: We appreciate the reviewer's detailed and positive evaluation of our work. We*  
209 *would like to thank the reviewer and have modified the manuscript according to the*  
210 *comments.*

211  
212 **INTRODUCTION**

213 L94 -95 Can you please give an example of the ranges of  $J_{max}:V_{max}$   
214 ratio found in these cited works to show how much it deviates from the normally  
215 adopted ratio of 2?

216 *Response: We have changed the text to read:*

217 *'However, recent studies have suggested the  $J_{max}:V_{cmax}$  ratio varies systematically across forest ecosystems and*  
218 *can range from 1 to 3 (Kattge and Knorr, 2007; Ellsworth et al., 2012; Kumarathunge et al., 2018)'*

219  
220 **METHODS**

221 L132: Is the repo unchanged or should the reader be directed to a certain  
222 commit version?

223 *Response: The repo will remain unchanged. Further development of the model will be*  
224 *through other branches of the repo.*

225  
226 L162: You do not introduce the variable D until line 172 and do not provide units.

227 *Response: We thank the reviewer for highlighting this, we have introduced D on line 155.*

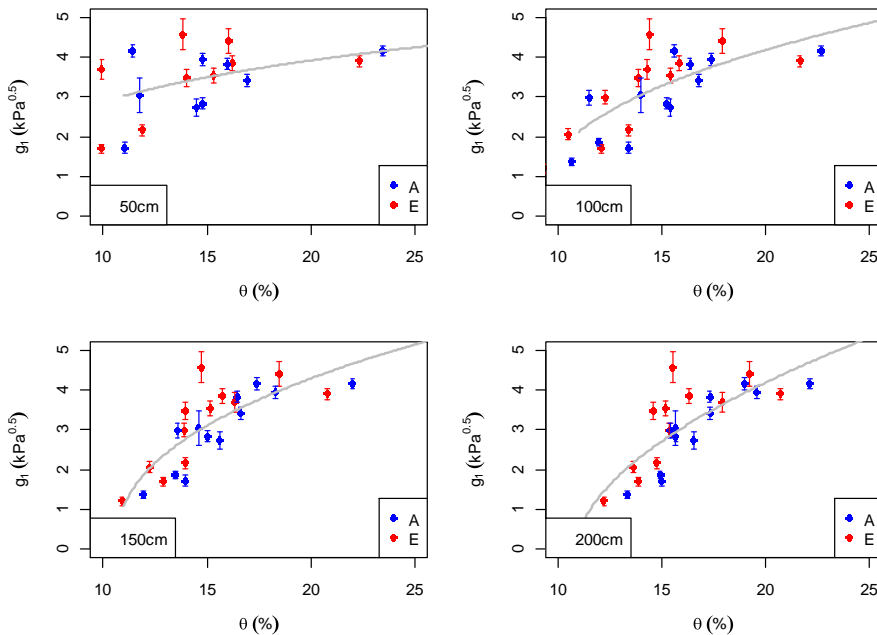
228



229 L164: Can you please clarify the choice between  $J_{max}$  and  $V_{cmax}$  here in the  $V_{max}$ ,  
 230  $t$  parameter?  
 231 *Response: There are measurements on  $J_{max25}$ ,  $V_{cmax25}$ , and their temperature dependence.*  
 232 *We correct  $J_{max25}$  and  $V_{cmax25}$  based on the leaf temperature to derive  $J_{max}$  and  $V_{cmax}$*   
 233 *following Eqn S5. These values of  $J_{max}$  and  $V_{cmax}$  are then reduced by VPD (a bit more*  
 234 *explanation....). We added reference to Text S1 in the manuscript.*

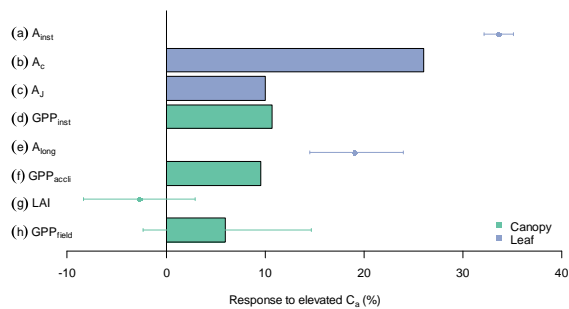
235  
 236 L175-177: I would introduce the equipment and measurement heights before the frequency,  
 237 but this is a minor point.  
 238 *Response: We have changed the ordering as suggested.*

239  
 240 L186: In Fig 2 you present that you use 150cm neutron probe measurements that were  
 241 conducted biweekly and linearly interpolated, but here you say these measurements  
 242 were not gap-filled? While I do not think this would majorly affect your results, averaging  
 243 the soil moisture over the entire 150 cm profile seems problematic as you are giving  
 244 equal weight to regions that are likely to contain significantly less root biomass. Would  
 245 it not be more fitting to use a weighted average based on the below-ground biomass  
 246 distribution to represent the soil moisture that the tree actually “feels”? Would this have  
 247 changed your  $g_1$ ?  
 248 *Response: We did not account for root distribution. Instead, we tested the  $g_1$  - SWC*  
 249 *relationship using SWC averaged over different depths and found that 150cm has the best fit.*  
 250 *This result is not shown in the paper but is as below.*



251  
 252  
 253 L202: Minor point of convention – normally see DBH represented in [cm]. I assume  
 254 you used DBH in [cm] in your allometry in Eq 4?  
 255 *Response: That was a typo and we have now fixed the unit to be cm, thanks.*

256  
257 L214-215: Fit statistics of this allometry?  
258 *Response: We have modified the sentence to read:*  
259 *'The values obtained via fitting for a and b were 492.6 and 1.8 respectively, with a root mean square error of*  
260 *14.4 m<sup>2</sup> and R<sup>2</sup> of 0.83'*  
261  
262 L225: No, no to citing an "in prep" when you seem to be presenting this data in this  
263 work.  
264 *Response: We replaced the "in prep" citation with Ellsworth et al. (2017) who also use*  
265 *these data. A much more detailed manuscript is in preparation and we had hoped to be able*  
266 *to cite that, but the 2017 citation is also appropriate.*  
267  
268 L278 Misspelling of ntheta\_min  
269 *Response: Thanks, this has been fixed.*  
270  
271 L246: Please expand up on the statement "within two weeks without rain" – was there  
272 some selection of points that happened based on this? I'm bit confused with the g1  
273 and soil moisture match up.  
274 *Response: We have modified the text to read:*  
275 *'The g<sub>1</sub> values were related to the nearest measurements of θ (within two weeks). In all cases, there has been no*  
276 *rainfall between g<sub>1</sub> and θ measurement dates. '*  
277  
278 L255: Missing commas.  
279 *Response: It was not clear to us what the reviewer is referring to.*  
280  
281 RESULTS  
282 The results presentation is somewhat difficult to follow given the large number  
283 of simulations and measurements spanning scales. Figure 4's mix of bar and point  
284 measurements is difficult to follow. Separating data measurements from modeled responses  
285 could help the reader follow better what is derived from models and what was  
286 an actual measured response. I appreciate the color coding between leaf and canopy  
287 measurements. Also, making a clearer distinction between the leaf-level models using  
288 the R package and the canopy scaled measures made using MAESPA would be  
289 helpful.  
290 *Response: We have changed the bottom row in fig4. Now all modelled results are in bars and*  
291 *observations in points. We have further clarified this in the caption. This should also help*  
292 *separate the results from leaf and canopy models.*  
293 *'The bars represent model outputs while points represent observations.'*



294

295

296 DISCUSSION

297 L397-398: I would love to see the timeseries that illustrates this stomatal closure at the  
 298 canopy scale.

299 *Response: These data were originally presented by Gimeno et al. (2016), who show a*  
 300 *timeseries in their Figure 2. The data themselves are also publicly available so that the*  
 301 *reader can make their own plots. See also Yang et al. (2019) who explore the relationship*  
 302 *with VPD.*

303

304

305 L405-418: Ah ha! This was the presentation of J:V ratio ranges that I was waiting for. I  
 306 would still suggest adding in a range to the introduction so that the reader is primed to  
 307 consider how variability in J:V could impact these modeled responses to eCa.

308 *Response: We have addressed this comment above.*

309 *'However, recent studies have suggested the  $J_{\text{max}}:V_{\text{cmax}}$  ratio varies systematically across forest ecosystems and*  
 310 *can range from 1 to 3 (Kattge and Knorr, 2007; Ellsworth et al., 2012; Kumarathunge et al., 2018)'*

311

312 L420: Yes, but would how would the way you averaged your soil moisture values affect  
 313 this value?

314 *Response: We think that the reviewer may have confused the convexity parameter  $\theta_j$  with soil*  
 315 *moisture content  $\theta$ . Unfortunately,  $\theta$  is the most commonly used symbol for the terms in both*  
 316 *fields. We edited the definition of the terms in Table 1 to clarify that values of theta, theta*  
 317 *max and theta min refer to soil moisture content.*

318

319 L449-451 I agree with this statement, but can you be more clear about what “uncertainty”  
 320 you are referring to? Are you talking about uncertainty in our forcing variables  
 321 for models; structural uncertainty in the models; both?

322 *Response: Here we specifically focused on the variability in the measurements (i.e., inter-*  
 323 *ring variability in this study). We clarified this further in the text:*

324 *'Secondly, the inherent ring-to-ring variation in this natural forest stand is even higher than the GPP response,*  
 325 *which highlights the importance of considering both the effect size and uncertainty in the observations than to*  
 326 *focus on statistical significance.'*

327

328 L462-463 Falsify those model simulations? Should we just throw the models in the trash or  
329 can we focus on an improvement in the model structure in order to capture these transitions  
330 between Rubisco limitation and RuBP regeneration? Or could it be also that there are other  
331 structural differences between those models and the explicit canopy structure of MAESPA?  
332 *Response: As the reviewer highlights, we are falsifying model assumptions, not the model as*  
333 *a whole. Thus, we do not advocate trashing the models, but rather we aim to identify ways*  
334 *forward for model improvement. We modified the text to read:*

335 *'With our results, it is possible to falsify some of the assumptions made in these model simulations and identify*  
336 *directions for model improvement.'*

337  
338 FIGURES

339 L708-711 Fig 2: You give no clear indication about what the different line colors mean.  
340 I assume these are replicates, but I am not clear about if these are elevated or control  
341 plots. You briefly mention ring numbers in text, but the figure would be improved if you  
342 make this distinction more visually apparent.

343 *Response: We apologise for the confusion. These details were inadvertently omitted from the*  
344 *caption. We now added*

345 *'Each line colour marks a different plot. Red colours show elevated CO<sub>2</sub> plots (treatment), while blue colours*  
346 *show ambient CO<sub>2</sub> plots (control).'*

347  
348 L714: "error bars represent standard error of fitted values" I'm a bit confused by this  
349 statement.

350 *Response: The observations were grouped by date and treatment before fitting. Only one g1*  
351 *was fitted to each group of data (as stated in the method section 23.3). As a result, the fitting*  
352 *has an uncertainty or error. We used standard error from each fitting to quantify the*  
353 *uncertainty. We added the following to the figure caption:*

354 *"g1 parameter values are fitted to data grouped by month and treatment."*

355  
356 L717: This figure is especially hard to follow and the mix of bar and points is difficult.  
357 I would suggest adding further groups to help identify measurements vs. leaf scale  
358 modeling vs. canopy scale modeling.

359 *Response: We have addressed this in the earlier comment from the reviewer. Now the bars*  
360 *represent model and points represent observations. We further clarified this in the caption.*

361

362  
363

1 **Low sensitivity of gross primary production to elevated CO<sub>2</sub> in a mature Eucalypt woodland**

2 **Authors:** Jinyan Yang<sup>1</sup>, Belinda E. Medlyn<sup>1</sup>, Martin G. De Kauwe<sup>2,3</sup>, Remko A. Duursma<sup>1</sup>, Mingkai Jiang<sup>1</sup>,  
3 Dushan Kumarathunge<sup>1</sup>, Kristine Y. Crous<sup>1</sup>, Teresa E. Gimeno<sup>4,5</sup>, Agnieszka Wujeska-Klause<sup>1</sup>, David S.  
4 Ellsworth<sup>1</sup>

5  
6 **Affiliation:** <sup>1</sup> Hawkesbury Institute for the Environment, Western Sydney University, Penrith, NSW, Australia

7 <sup>2</sup> ARC Centre of Excellence for Climate Extremes, Sydney, NSW 2052, Australia

8 <sup>3</sup> Climate Change Research Centre, University of New South Wales, Sydney, NSW 2052, Australia

9 <sup>4</sup> Basque Centre for Climate Change, Scientific Campus of the University of the Basque Country, Leioa, Spain

10 <sup>5</sup> IKERBASQUE, Basque Foundation for Science, 48008, Bilbao, Spain

11 Correspondence to: Jinyan Yang ([jinyan.yang@westernsydney.edu.au](mailto:jinyan.yang@westernsydney.edu.au))

12

13

14

15 **For submission to: Biogeosciences Discussions**

16 No of words in abstract: 269

17 No of words in main text: 6705

18 No of Figures: 8

19 No of Tables: 1

20

21

22 **Abstract**

23 The response of mature forest ecosystems to rising atmospheric carbon dioxide concentration ( $C_a$ ) is a major  
24 uncertainty in projecting the future trajectory of the Earth's climate. Although leaf-level net photosynthesis is  
25 typically stimulated by exposure to elevated  $C_a$  ( $eC_a$ ), it is unclear how this stimulation translates into carbon  
26 cycle responses at whole-ecosystem scale. Here we estimate a key component of the carbon cycle, the gross  
27 primary productivity (GPP), of a mature native Eucalypt forest exposed to Free Air  $CO_2$  Enrichment (the  
28 EucFACE experiment). In this experiment, light-saturated leaf photosynthesis increased by 19% in response to a  
29 38% increase in  $C_a$ . We used the process-based forest canopy model, MAESPA, to upscale these leaf-level  
30 measurements of photosynthesis with canopy structure to estimate ~~Gross Primary Production (GPP)~~ and its  
31 response to  $eC_a$ . We assessed the direct impact of  $eC_a$ , as well as the indirect effect of photosynthetic  
32 acclimation to  $eC_a$  and variability among treatment plots via different model scenarios.

33 At the canopy scale, MAESPA estimated a GPP of  $1574 \text{ g C m}^{-2} \text{ yr}^{-1}$  under ambient conditions across four years  
34 and a direct increase in GPP of +11% in response to  $eC_a$ . The smaller canopy-scale response simulated by the  
35 model, as compared to the leaf-level response, could be attributed to the prevalence of RuBP-regeneration  
36 limitation of leaf photosynthesis within the canopy. Photosynthetic acclimation reduced this estimated response  
37 to 10%. After taking in account the baseline variability in leaf area index across plots, we estimated a field GPP  
38 response to  $eC_a$  of 6% with a 95% confidence interval (-2, 14%). These findings highlight that the GPP response  
39 of mature forests to  $eC_a$  is likely to be considerably lower than the response of light-saturated leaf  
40 photosynthesis. Our results provide an important context for interpreting  $eC_a$  responses of other components of  
41 the ecosystem carbon cycle.

## 42 1. Introduction

43 Forests represent the largest long-term terrestrial carbon storage (Bonan, 2008; Pan et al., 2011). Atmospheric  
44 carbon dioxide concentration ( $C_a$ ) has increased significantly since the beginning of the industrial era (Joos and  
45 Spahni, 2008), but the increase would have been considerably larger without forest carbon sequestration, which  
46 is estimated to have offset 25-33% of recent anthropogenic  $CO_2$  emissions (Le Quéré et al. 2017).  $C_a$  is projected  
47 to continue to increase by 1-5  $\mu\text{mol mol}^{-1}$  per year into the future (IPCC, 2014), but the rate of this rise depends  
48 on the magnitude of the forest feedback on  $C_a$ . At the leaf scale, the direct physiological effects of rising  $C_a$  are  
49 well understood: elevated  $C_a$  ( $eC_a$ ) stimulates plant photosynthesis (Kimball et al. 1993; Ellsworth et al. 2012)  
50 and reduces stomatal conductance (Morison, 1985, Saxe et al. 1998), which together increase leaf water-use  
51 efficiency (De Kauwe et al. 2014). These physiological responses at [the leaf scale can increase ecosystem](#)  
52 [carbon uptake, which in turn may result in increased carbon storage in the ecosystem, mitigating against the rise](#)  
53 [in  \$C\_a\$](#) . However, projecting the response of the terrestrial carbon sink to future increases in  $C_a$  is a major  
54 uncertainty in models (Friedlingstein et al. 2014), highlighting an urgent need to make greater use of data from  
55 manipulative experiments at leaf scale to inform terrestrial biosphere models (Medlyn et al., 2015).

56 Our understanding of ecosystem responses to  $eC_a$  relies on both experiments and observations. However, results  
57 from different types of studies show some important areas of disagreement ([Fatichi et al., 2019](#)). At the global  
58 scale, satellite data provide evidence of a strong greening trend over the last 20 years, indicating an increase in  
59 leaf area and/or above-ground biomass, which has been attributed to the gradual increase in  $CO_2$  (Donohue et  
60 al., 2009; Donohue et al., 2013; Yang et al., 2016; Zhu et al., 2016). A positive response of carbon  
61 uptake/greenness is also found in manipulative  $eC_a$  open-top chamber experiments with young trees (Eamus and  
62 Jarvis, 1989; Curtis and Wang 1998; Saxe et al. 1998; Medlyn et al., 1999) and ecosystem-scale FACE  
63 experiments in young, aggrading forest stands (Ainsworth and Long, 2005; Norby et al., 2005; , Ellsworth et al.  
64 2012; Walker et al. 2019). In contrast, individual-tree experiments with mature trees (>30 years old) have found  
65 relatively small responses of tree growth to  $eC_a$  despite an apparent increase in leaf photosynthesis (Dawes et  
66 al., 2011; Sigurdsson et al., 2013; Klein et al., 2016). Also, tree-ring studies indicate an apparent lack of  
67 stimulation of vegetation growth in mature forests over the last century (Peñuelas et al. 2011; Silva and Anand,  
68 2013; van der Sleen et al. 2014). These studies raise important questions about how mature ecosystems will  
69 respond to  $eC_a$ .

70 The Eucalyptus FACE experiment (EucFACE; Australia) is the first replicated, ecosystem-scale experiment  
71 where a mature native forest has been experimentally subjected to  $eC_a$  and provides a valuable case study to  
72 assess the response of a mature forest response to  $eC_a$  under field conditions (Ellsworth et al. 2017). Results  
73 from the first five years (2013-2018) of leaf gas exchange measurements showed a consistent stimulation of  
74 leaf-level light-saturated net photosynthesis ( $A$ ) of 19% (Ellsworth et al., 2017; Wujeska-Klaue et al., 2019).  
75 Nevertheless, the increase in  $A$  did not lead to a detectable change in above-ground growth (Ellsworth et al.,  
76 2017). These experimental results are consistent with empirical evidence arising from tree-ring studies  
77 (Peñuelas et al. 2011; Silva and Anand, 2013; van der Sleen et al. 2014) and also with experimental evidence  
78 from individual mature trees (Körner et al., 2005; Dawes et al., 2011; Klein et al., 2016).

79 As a first step towards reconciling the  $eC_a$  responses of leaf photosynthesis and above-ground growth in this  
80 experiment, here we quantify how the whole canopy carbon uptake, or gross primary productivity (GPP) was  
81 increased under  $eC_a$ . The response of GPP is important because it provides ~~an upper bound a reference point and~~  
82 ~~possibly the upper bound on~~ against which to compare the ~~potential~~ response of other components of ecosystem  
83 carbon balance, such as above-ground growth. It needs to be quantified explicitly because the response of GPP  
84 to  $eC_a$  may be quite different to that of leaf net photosynthesis. The leaf-level response of photosynthesis to  $eC_a$   
85 is usually measured on sunlit leaves under saturating light (Ainsworth and Rogers, 2007). As a result, these leaf-  
86 level  $eC_a$  responses largely reflect the responses of the photosynthesis rate when limited by maximum Rubisco  
87 activity ( $V_{\text{cmax}}$ ). However, depending on the canopy architecture and ambient light condition, the canopy could  
88 have many shaded leaves, which would mean that the emergent rate of photosynthesis could actually be limited  
89 by RuBP regeneration ( $J$ ). RuBP-regeneration limited photosynthesis has a smaller response to  $eC_a$  than  
90 Rubisco-limited photosynthesis (Ainsworth and Rogers, 2007), resulting in a smaller response of GPP than leaf  
91 photosynthesis under saturating light.

92 The transition from RuBP-regeneration to Rubisco-limited photosynthesis of the canopy is determined by the  
93 ratio of the maximum capacities for RuBP-regeneration and Rubisco activity,  $J_{\text{max}}$  and  $V_{\text{cmax}}$  (Friend, 2001;  
94 Zaehle et al. 2014; Rogers et al., 2017). Wullschleger (1993) reported a  $J_{\text{max}}:V_{\text{cmax}}$  ratio of 2, which has been  
95 widely adopted in models (e.g., Wang et al., 1998; Luo et al., 2001; Rogers et al., 2017). However, recent  
96 studies have suggested the  $J_{\text{max}}:V_{\text{cmax}}$  ratio varies systematically across forest ecosystems and can range from 1  
97 to 3 (Kattge and Knorr, 2007; Ellsworth et al., 2012; Kumarathunge et al., 2018). A lower  $J_{\text{max}}:V_{\text{cmax}}$  ratio results  
98 in more frequent RuBP-regeneration limitation of photosynthesis, which reduces the response of GPP to  $eC_a$ .

99 It is difficult to directly measure the  $eC_a$  effect on GPP. In some previous  $eC_a$  experiments, GPP has been  
100 estimated by scaling up from leaf-level measurements using a canopy model. Wang et al (1998) and Luo et al  
101 (2001) both used the tree array model, MAESPA, which can simulate the radiative transfer within and between  
102 tree crowns and can be parameterised to describe the spatial locations and sizes of trees in  $eC_a$  experiments. In  
103 these previous applications of MAESPA, the direct response of GPP to  $eC_a$  was consistently half of that  
104 observed at the leaf level because of a large contribution of RuBP-regeneration limited photosynthesis to GPP  
105 (Wang et al., 1998; Luo et al., 2001). However, the direct effect of  $eC_a$  on photosynthesis was modified by two  
106 major indirect effects. When LAI increased under  $eC_a$ , the additional leaf area amplified the GPP response by up  
107 to 60%. The other factor is the downregulation of photosynthesis under  $eC_a$ , or photosynthetic acclimation  
108 (Long et al., 2004; Ainsworth and Rogers, 2007; Rogers, et al., 2017). Under long-term exposure to  $eC_a$ , some  
109 plants have been observed to reduce nitrogen allocation to Rubisco, which results in a decrease of  
110 photosynthetic capacity (Gunderson and Wullschleger, 1993). The average decrease of  $V_{\text{cmax}}$  among plants in  
111 FACE experiments was found to be 13% for all species and 6% for trees (Ainsworth and Long, 2005). Both  
112 Wang et al. (1998) and Luo et al. (2001) tested the impact of photosynthetic acclimation and showed a moderate  
113 reduction of canopy GPP (5-6%) due to photosynthetic acclimation (10-20%) at the studied experiments.

114 Following Wang et al. (1998) and Luo et al. (2001), we used MAESPA (Duursma and Medlyn, 2012) to  
115 estimate canopy GPP at EucFACE in ambient and elevated  $C_a$  treatments. The model has previously been  
116 evaluated with leaf- and whole-tree- scale measurements from EucFACE (Yang et al., in review). Here, we first  
117 parameterised the model with physiological, and structural and meteorological data measured during the



118 experiment. Then, we quantified the response of canopy GPP to  $eC_a$  and partitioned this response into the direct  
119 stimulation of GPP and the indirect effects of photosynthetic acclimation and variation of LAI. The overall goal  
120 of this study was to estimate the magnitude of the response of forest canopy GPP to  $eC_a$  in order to provide a  
121 baseline against which to compare changes in other components of the ecosystem carbon balance.

## 122 2. Methods

### 123 2.1 Site

124 The EucFACE experiment (technical details in Gimeno et al., 2016) is located in western Sydney, Australia  
125 (33.617S, 150.741E). It consists of six circular plots, each of which has a diameter of 25 m, enclosing 15-25  
126 mature forest trees (referred to as 'rings' hereafter). The rings are divided into two groups: control (with ambient  
127  $C_a$ ; 390-400  $\mu\text{mol mol}^{-1}$  during the study period) and experimental ( $eC_a$ ; +150  $\mu\text{mol mol}^{-1}$ ). The tree canopy is  
128 dominated by *Eucalyptus tereticornis* Sm. which are ~20 m in height and have a basal area of ~24  $\text{m}^2 \text{ha}^{-1}$ . The  
129 site receives a mean annual precipitation of 800  $\text{mm yr}^{-1}$ , a mean annual photosynthetically active radiation  
130 (PAR) of 2600  $\text{MJ m}^{-2} \text{yr}^{-1}$ , and a mean annual temperature of 17 °C.

### 131 2.2 Model

132 The MAESPA model is a process-based tree-array model (Wang and Jarvis, 1990) that calculates canopy carbon  
133 and water exchange ([https://bitbucket.org/remkoduursma/maespa/src/Yang\\_et\\_al\\_2019/](https://bitbucket.org/remkoduursma/maespa/src/Yang_et_al_2019/)). At each 30-minute  
134 timestep, the model simulates the radiative transfer, photosynthesis, and transpiration of individual trees  
135 mechanistically. Soil moisture balance can be calculated dynamically, but here we chose to improve accuracy by  
136 using soil moisture as an input to the model (Duursma and Medlyn, 2012).

137 The model represents the tree canopy as an array of tree crowns. The location and dimensions of each crown are  
138 specified based on-site measurements (see 2.3.2 Canopy structure, below). Calculations of carbon and water  
139 fluxes are made for each tree crown, which is divided into six layers. Here it was assumed that crowns are  
140 represented by an ellipsoidal shape and that leaf area is uniformly distributed across layers within the tree  
141 crown. The leaf angles were assumed to follow a spherical distribution to ensure consistency with the method  
142 used to estimate leaf area index (LAI) in Duursma et al. (2016). Within each layer, the model evaluates the  
143 radiation transfer and leaf gas exchange at 12 grid points such that each crown is represented by a total of 72  
144 grid points. The radiation intercepted at each grid point is calculated for direct and diffuse components by  
145 considering shading from the upper crown and surrounding trees and solar angle (zenith and azimuth), and light  
146 source (diffuse or direct). Penetration by direct radiation to each grid point is used to estimate the sunlit and  
147 shaded leaf area at each grid point. The radiation intercepted by the fraction of sunlit and shade foliage is then  
148 used to calculate the leaf gas exchange.

149 The gas exchange sub-model combines the leaf photosynthesis model of Farquhar et al. (1980) with the stomatal  
150 optimisation model, following Medlyn et al. (2011). Stomatal conductance is modelled as:

$$151 \quad g_s = 1.6 \cdot \left(1 + \frac{g_1}{\sqrt{D}}\right) \cdot \frac{A_{\text{net}}}{c_a} \quad (1)$$

152 where  $g_s$  is the stomatal conductance to water vapour ( $\text{mol m}^{-2} \text{s}^{-1}$ );  $g_1$  is a parameter that represents the  $g_s$   
153 sensitivity to photosynthesis ( $\text{kPa}^{0.5}$ ; see definition in Medlyn et al., (2011));  $A_{\text{net}}$  is the net  $\text{CO}_2$  assimilation rate

154 ( $\mu\text{mol m}^{-2} \text{s}^{-1}$ );  $C_a$  is the atmospheric  $\text{CO}_2$  concentration ( $\mu\text{mol mol}^{-1}$ ) and  $D$  is the vapour pressure deficit  
155 (kPa). The factor 1.6 converts the conductance of  $\text{CO}_2$  to that of  $\text{H}_2\text{O}$ .

156 The impact of soil moisture on  $g_s$  is represented through an empirical function that links soil water availability  
157 to  $g_1$  following (Drake et al., 2017):

$$158 \quad g_1 = g_{1,max} \left( \frac{\theta - \theta_{min}}{\theta_{max} - \theta_{min}} \right)^q \quad (2)$$

159 where the  $g_{1,max}$  is the maximum  $g_1$  value;  $\theta$  is volumetric soil water content (%);  $\theta_{max}$  and  $\theta_{min}$  are the upper and  
160 lower limit within which  $\theta$  has impact on  $g_1$ ;  $q$  describes the non-linearity of the curve. The equations to  
161 calculate  $A_{net}$  are in Supplementary (Text S1, Eqns. S1 – S6).

162 Following Yang et al. (2019), MAESPA considers a non-stomatal limitation to biochemical parameters  $J_{max}$  and  
163  $V_{cmax}$  at high  $D$ :

$$164 \quad V_{max} = V_{max,t} (1 - c_D \cdot D) \quad (3)$$

165 where  $V_{max,t}$  is the  $J_{max}$  or  $V_{cmax}$  at given leaf temperature (Text S1), and  $c_D$  is a fitted parameter (Table 1). This  
166 relationship is empirical and fitted to data collected in EucFACE. Incorporating this relationship was shown to  
167 improve the predicted photosynthesis by the leaf gas exchange model (Yang et al., 2019).

168 Combining Eqns. 1- 3 and S1 – S6 yields the  $g_s$  and  $A_{net}$  of each grid point, which is then multiplied by leaf area  
169 at each grid point and summed to give whole-tree photosynthesis. Photosynthesis of individual trees is then  
170 summed to give whole-canopy photosynthesis.

## 171 2.3 Model Parameterisation

### 172 2.3.1 Meteorological forcing

173 The model is driven by *in situ* PAR, wind speed, air temperature, vapour pressure deficit ( $D$ ), and soil  
174 moisture measurements from 2013 to 2016 (Figures 1 and 2). Each ring has a set of PAR (LI-190, Li-cor,  
175 Lincoln, NE, U.S.), wind speed (Wincap Ultrasonic WMT700 Vaisala, Vantaa, Finland), humidity, and  
176 temperature sensors (HUMICAP® HMP 155 Vaisala, Vantaa, Finland) at the centre of the ring above the  
177 canopy at 23.5 m. The PAR, air temperature, and relative humidity were measured every five minutes in each  
178 ring and then were gap-filled by linear interpolation and aggregated to 30 minute-mean time slices across all six  
179 rings (Figure 1). Each ring has a set of PAR (LI-190, Li-cor, Lincoln, NE, U.S.), wind speed (Wincap Ultrasonic  
180 WMT700 Vaisala, Vantaa, Finland), humidity, and temperature sensors (HUMICAP® HMP 155 Vaisala,  
181 Vantaa, Finland) at the centre of the ring above the canopy at 23.5 m.  $D$  was calculated from temperature and  
182 humidity measurements.

183 Two levels of  $C_a$  were used in the model according to the measured  $C_a$  (LI-840, Li-cor, Lincoln, NE, U.S.). The  
184 ambient  $C_a$  was gap-filled (in total <10 days during four years gaps due to power outage) and aggregated to 30  
185 minute-mean time slices from the five-minute measurements across the three ambient rings (rings 2, 3, and 6).  
186 The  $eC_a$  was processed in the same way but using data from the experimental rings (rings 1, 4, and 5).

187 The volumetric soil water content ( $\theta$ ) was used as an estimate of plant water availability and was taken every 20  
188 days using neutron measurements at 25 cm intervals (503DR Hydroprobe, Instroteck, NC, U.S.) and averaged to  
189 the top 150 cm (Figure 2). There were two probes in each ring and the average of these probes was used to

Formatted: Font: Italic

190 represent the ring average for each measurement date.  $\theta$  was updated on the days of measurements and thus not  
191 gap-filled.

### 192 2.3.2 Canopy structure

193 Trees in MAESPA were represented by their actual location, height, and crown size to mimic the realistic  
194 effects of shading. Tree location, crown height, crown base and stem diameter were measured in January 2013  
195 at the start of the experiment. For each ring, a time-series of LAI was obtained based on measurements of  
196 above- and below- canopy PAR (Duursma et al. 2016). This LAI represents plant area index, which includes the  
197 woody component as well as leaves and does not account for clumping. In order to retrieve the actual LAI, we  
198 assumed a constant branch and stem cover ( $0.8 \text{ m}^2 \text{ m}^{-2}$ ) based on the lowest LAI during November 2013 when  
199 the canopy shed almost all leaves. The LAI used in this study was thus the plant area index estimates from  
200 Duursma et al. (2016), less  $0.8 \text{ m}^2 \text{ m}^{-2}$  (Figure 2a). Since LAI is the only parameter beside soil moisture that  
201 differed by ring, canopy structure (i.e., the LAI and its distribution) was the major driver of inter-ring  
202 variability.

203 The total leaf area ( $\text{m}^2$ ) of each ring was calculated as the product of LAI and ground area of each plot ( $491 \text{ m}^2$ ).  
204 This total leaf area (LA) was then assigned to each tree based on an allometric relationship between the total leaf  
205 area ( $\text{m}^2$ ) and diameter at breast height (DBH;  $\text{cm}$ ). The allometric relationship was derived from data in the  
206 BAAD database (Falster et al., 2015) for *Eucalyptus* trees grown in natural conditions with DBH <1 m to match  
207 the characteristics of EucFACE. In total, this database yielded a total of 66 observations with which to estimate  
208 the relationship between LA and DBH:

$$209 L_{allom} = a \cdot DBH^b \quad (4)$$

210 where  $L_{allom}$  is the theoretical leaf area based on allometric relationship to DBH. The values obtained via fitting  
211 for  $a$  and  $b$  were 492.6 and 1.8 respectively, with a root mean square error of  $14.4 \text{ (m}^2)$  and correlation  
212 coefficient of 0.83. This Eqn. 4 relationship was used to assign the total LA of each ring to each tree in the  
213 following steps: (i) the  $L_{allom}$  for each tree was calculated based on DBH; (ii) the  $L_{allom}$  was summed to obtain a  
214 total LA for each ring; and (iii) the fractional contribution of each tree to the ring total LA was calculated. The  
215 total LA based on LAI was then assigned to each tree based on this fraction.

216 The crown radius was calculated with a linear function with DBH based on measurements made in August  
217 2016. The data consisted of DBH and crown radius (one on North-South axis and one on East-west axis) of four  
218 trees in each ring. The crown radius measurements were averaged by tree and used to fit a linear model with  
219 DBH. The estimated slope and intercept of the relationship are  $0.095 \text{ (m cm}^{-1})$  and  $0.765 \text{ (m)}$ , respectively.

220 MAESPA also considered the shading from surrounding trees outside the rings. However, no measurements of  
221 locations or diameters were available for the trees surrounding the rings. Therefore, a total of 80 surrounding  
222 trees were arbitrarily assumed to form two uniform and circular layers around each ring. They were assigned the  
223 mean height, mean crown radius, and mean leaf area estimated from all trees in EucFACE. Except for shading,  
224 the surrounding trees have no impact on the trees within the rings. Ring 1 is shown in Figure S1 as an example  
225 of the representation of canopy structure in MAESPA.

### 226 2.3.3 Physiology

227 The physiological parameters were estimated from field gas exchange measurements as described below. The  
228 data were collected with portable photosynthesis systems (Li-6400, Li-Cor, Inc., USA). The only parameter  
229 found to differ between ambient and elevated  $C_a$  rings was  $V_{cmax,25}$  ( $V_{cmax}$  at 25 °C; Ellsworth et al., [in  
230 prep2017](#)). Hence, all other parameters (e.g., the temperature responses of photosynthesis and respiration) were  
231 estimated by combining all data across  $CO_2$  treatments. Fitted parameter values are given in Table 1.

232 A set of temperature-controlled photosynthesis- $CO_2$  response ( $A-C_i$ ) curves was measured at different leaf  
233 temperatures (20–40 °C) under saturating light in February 2016. The dataset was used to quantify the  
234 temperature dependences of  $J_{max}$  and  $V_{cmax}$  by fitting a peaked Arrhenius function (Eqn. S5) to the  
235 measurements. We assumed that these temperature response functions applied throughout the period of the  
236 study.

237 Light- and temperature-controlled  $A-C_i$  curves were also measured in the morning for ten field campaigns  
238 during 2013 to 2016. All  $A-C_i$  curves were started at the growth  $C_a$  of 395  $\mu\text{mol mol}^{-1}$  or 545  $\mu\text{mol mol}^{-1}$   
239 (depending on  $eC_a$  treatment) with a saturating light of 1800  $\mu\text{mol m}^{-2} \text{s}^{-1}$  and a flow rate of 500  $\mu\text{mol s}^{-1}$  with  
240 temperature controlled to a constant based on the seasonal temperature. These data were used to estimate  $J_{max}$   
241 and  $V_{cmax}$  at 25 °C using the *fitaci* function in the *plantecophys* R package (Duursma, 2015), using the measured  
242 temperature responses of  $J_{max}$  and  $V_{cmax}$  described in the previous paragraph to correct to 25 °C.

243 Repeated gas exchange measurements were made on the same leaves in the morning and afternoon under  
244 prevailing field conditions and saturating light (photon flux density = 1800  $\mu\text{mol m}^{-2} \text{s}^{-1}$ ) on four occasions in  
245 2013 (“diurnal”; Gimeno et al., [20162015](#)). To expand the diurnal dataset, we obtained the points from  $A-C_i$   
246 curves at field  $C_a$  and combined the two data sets. These data were used to estimate the  $g_1$  parameter in the  
247 stomatal conductance model (Eqn. 1) using the *fitBB* function in the *plantecophys* R package (Duursma, 2015).  
248 One  $g_1$  value was fitted to the data from each treatment and date. The  $g_1$  values were then regressed against  $\theta$   
249 measured in each treatment group to estimate the impact of soil moisture availability on leaf gas exchange,  
250 following Eqn. 2. The  $g_1$  values were related to the nearest measurements of  $\theta$  (within two weeks ~~without rain~~).  
251 [There has been no rainfall between  \$g\_1\$  and  \$\theta\$  measurement dates](#). Eqn. 2 was fitted to this data set using the non-  
252 linear least squares method (Figure 3).

253 The dark respiration rate of foliage,  $R_{dark}$ , was measured at least three hours after sunset at a range of leaf  
254 temperatures (14–60 °C) in February 2016 also with LiCor 6400. The temperature dependence of  $R_{dark}$  was fitted  
255 using non-linear least squared method to all of the measured data using Eqn. S6. Light responses of  
256 photosynthesis were measured on two trees from each ring in October 2014 (Crous et al., unpublished). This  
257 data set was used to constrain the light response parameters ( $\alpha_j$  and  $\theta_j$ ) in Eqn. S4. Details of fitting the light  
258 response curves are provided in supplementary (Text S1).

#### 259 2.4 Model simulations and analysis

260 MAESPA was used to simulate radiation interception and gas exchange of all six rings between 1 January 2013  
261 and 31 December 2016 on a half-hourly basis. The model simulated half-hourly gross primary production (GPP)  
262 of each tree, which was then summed for all trees in each ring to get the total annual GPP for each ring and year.

263 Four different sets of simulations were used to estimate carbon uptake under ambient and  $eC_a$  and to identify the  
264 key limiting factors on canopy GPP response to  $eC_a$ . Firstly, we carried out a simulation of leaf scale (“leaf

265 scenario”) photosynthesis with measured meteorological data but fixed physiological data ( $g_1 = 3.3 \text{ kPa}^{0.5}$ ,  
 266  $V_{\text{cmax},25} = 91 \text{ } \mu\text{mol m}^{-2} \text{ s}^{-1}$ , and  $J_{\text{max},25} = 159 \text{ } \mu\text{mol m}^{-2} \text{ s}^{-1}$ ). This simulation aimed to quantify the  $\text{CO}_2$  response of  
 267 Rubisco-limited and RuBP-limited photosynthesis at the leaf scale. This calculation was made using the  
 268 *photosyn* function in *plantecophys* R package (Duursma, 2015). This function implements the leaf gas exchange  
 269 routine used in MAESPA.

270 Secondly, MAESPA was run for all six rings with ambient  $C_a$  and with  $V_{\text{cmax},25}$  from ambient measurements  
 271 (“ambient scenario”). The results of this simulation were used to calculate the GPP of each ring under ambient  
 272 conditions. The ambient GPP values were also used to evaluate the inherent variability among the rings.

273 Thirdly, all six rings were simulated with  $eC_a$  and  $V_{\text{cmax},25}$  based on measurements from ambient rings (“elevated  
 274 scenario”). The results of this simulation were compared to those from the ambient scenario to illustrate the  
 275 instantaneous response of canopy GPP to  $eC_a$  in each ring and year. This simulation also quantifies the variation  
 276 of the GPP response to  $eC_a$  across rings and years.

277 Lastly, we simulated the response of the three rings exposed to  $eC_a$  (rings 1, 4, and 5) using the  $V_{\text{cmax},25}$  and  $eC_a$   
 278 measured from these elevated rings (“field scenario”). Results from the field scenario were used for two  
 279 analyses: (i) to compare GPP from the field scenario to that of the three rings from the elevated scenario (i.e.,  
 280  $eC_a$  and ambient  $V_{\text{cmax},25}$ ), which allows us to quantify the impact of photosynthetic acclimation (i.e., due to a  
 281 reduction in  $V_{\text{cmax}}$ ); (ii) to calculate the difference in GPP between the three ambient rings in ambient scenario  
 282 and elevated rings in the field scenario to estimate the response of GPP to  $eC_a$  in the field.

283 *Table 1. Summary table of parameter definitions, units, and sources used in this study.*

Parameters	Definitions	Units	Values	Eqn.
$\alpha_j$	Quantum yield of electron transport rate	$\mu\text{mol electron } \mu\text{mol}^{-1} \text{ photon}^{-1}$	0.30	S7
$a$	Fitted slope of LA and DBH	$\text{m}^2 \text{ m}^{-1}$	492.6	4
$a_{\text{abs}}$	Absorptance of PAR	fraction	0.825	S4
$b$	Fitted index of LA and DBH	-	1.8	4
$c_D$	Slope of $V_{\text{cmax}}$ to $D$	$\text{kPa}^{-1}$	0.14	3
$\Delta S$	Entropy factor	$\text{J mol}^{-1} \text{ K}^{-1}$	639.60 ( $V_{\text{cmax}}$ ); 638.06 ( $J_{\text{max}}$ )	S5
$E_a$	Activation energy	$\text{J mol}^{-1}$	66386 ( $V_{\text{cmax}}$ ); 32292 ( $J_{\text{max}}$ )	S5
$g_{1,\text{max}}$	Maximum $g_1$ value	$\text{kPa}^{0.5}$	5.0	2
$H_d$	Deactivation energy	$\text{J mol}^{-1}$	200000	S5
$\theta_j$	Convexity of electron transport rate to $Q_{\text{APAR}}$	-	0.48	S8
$\theta_{\text{max}}$	Upper limit <del>which of soil water content above which <math>g_1</math> is maximum <math>\theta</math> has impact on <math>g_1</math></del>	-	0.240	2
$\theta_{\text{min}}$	Lower limit <del>of soil water content below which <math>g_1</math> is zero which <math>\theta</math> has impact on <math>g_1</math></del>	-	0.106	2
$J_{\text{max},25}$	Value of $J_{\text{max}}$ at 25°C	$\mu\text{mol electron m}^{-2} \text{ s}^{-1}$	159	3
$k_T$	Sensitivity of $R_{\text{dark}}$ to temperature	$^{\circ}\text{C}^{-1}$	0.078	S6
$q$	The non-linearity of the $g_1$ dependence of $\theta$	-	0.425	2
$R_{\text{day},25}$	Light respiration rate	$\mu\text{mol C m}^{-2} \text{ s}^{-1}$	0.9	S6
$R_{\text{dark},25}$	Dark respiration rate	$\mu\text{mol C m}^{-2} \text{ s}^{-1}$	1.3	S6
$R_{\text{gas}}$	Gas constant	$\text{J mol}^{-1} \text{ K}^{-1}$	8.314	S5

$V_{\text{cmax},25}$	Value of $V_{\text{cmax}}$ at 25°C	$\mu\text{mol C m}^{-2} \text{ s}^{-1}$	91 (ambient); 83 (elevated)	3
----------------------	------------------------------------	---	--------------------------------	---

284

285

### 3. Results

286

Figure 4 summarises the results from measurements and the different simulations conducted in this study. It demonstrates that the impact of  $eC_a$  diminishes as calculations are scaled from the instantaneous leaf-level response ( $A_{\text{inst}}$ ) to the long-term canopy response ( $GPP_{\text{field}}$ ) and the various feedback effects are accounted for. Each row of Figure 4 is explained in detail in the following paragraphs.

287

288

289

290

#### 3.1 Instantaneous $C_a$ response of photosynthesis at leaf and canopy scale

291

The mean instantaneous  $C_a$  response of leaf-level photosynthesis ( $A_{\text{inst}}$ ) was +33% (Figure 4a). This response ratio was calculated from ~600 light- and temperature-controlled  $A-C_i$  curves measured in the ambient rings.

292

293

From the curves, we extracted the photosynthesis at 400 and 550  $C_a$  ( $\mu\text{mol mol}^{-1}$ ) and calculated the instantaneous  $C_a$  effect as their ratio. This approach allows an estimation of the direct  $\text{CO}_2$  response independent of the impact of photosynthetic acclimation.

294

295

296

By contrast, the modelled direct GPP response to  $eC_a$  was considerably less, just +11%, as shown in Figure 4d (“GPP<sub>inst</sub>”). This canopy response rate was calculated by comparing the modelled GPP of all six rings under ambient and elevated  $C_a$  (“ambient” vs. “elevated” scenario). As a result, this direct canopy GPP response also excludes the impact of photosynthetic acclimation.

297

298

299

300

Our results show that the major reason for the difference between the direct leaf and canopy photosynthesis responses to  $eC_a$  is the relative contributions from Rubisco- and RuBP-regeneration-limited photosynthesis (cf. Figure 4 b and c). Figure 5 shows that the response of photosynthesis to  $eC_a$  is considerably higher when Rubisco activity limits photosynthesis ( $A_c$ ) than when RuBP-regeneration limits photosynthesis ( $A_j$ ). When averaged over the range of leaf temperatures experienced during the four years of experiment, the  $A_c$  response to  $eC_a$  on average (+26%; Figure 4b) is larger than that of  $A_j$  (+10%; Figure 4c). Leaf gas exchange measurements were taken in saturating light ( $1800 \mu\text{mol m}^{-2} \text{ s}^{-1}$ ) and thus, are mostly Rubisco limited. The observed response rate of  $A_{\text{inst}}$  is thus close to that of  $A_c$ .

301

302

303

304

305

306

307

308

At the canopy scale, a large fraction of the modelled canopy photosynthesis is limited by RuBP-regeneration. In Figure 6, we show the distribution of  $A_c$  and  $A_j$  during the four years of simulation as calculated by MAESPA. On average, 70% of the canopy photosynthesis is limited by RuBP-regeneration under ambient conditions (“ambient scenario”). The high fraction of  $A_j$  is partly a consequence of the relatively low ratio of  $J_{\text{max},25}$  to  $V_{\text{cmax},25}$  ( $J:V$  ratio) which was estimated to be 1.7 (Table 1). In Figure 7, we estimated the PAR level at which Rubisco activity becomes limiting to leaf photosynthesis. The transition point from Rubisco- to RuBP-regeneration-limited photosynthesis was calculated from the leaf gas exchange sub-model by assuming a constant  $C_a$  ( $390 \mu\text{mol mol}^{-1}$ ),  $D$  (1.5 kPa),  $g_l$  ( $3.3 \text{ kPa}^{0.5}$ ), and  $V_{\text{cmax},25}$  ( $90 \mu\text{mol m}^{-2} \text{ s}^{-1}$ ) but varying leaf temperature. As shown, under these conditions, when temperature = 25 °C and  $J:V$  ratio = 1.7, Rubisco activity limits photosynthesis only when incident PAR >  $1800 \mu\text{mol m}^{-2} \text{ s}^{-1}$ . Using a higher  $J:V$  ratio such as the commonly-used value of 2 would decrease the saturating PAR value at which photosynthesis becomes Rubisco

309

310

311

312

313

314

315

316

317

318

319 limited. We ran additional simulations assuming a J:V ratio of 2 and found that, with this ratio, MAESPA  
320 estimated 48% of photosynthesis to be RuBP-regeneration limited under ambient conditions and a direct GPP  
321 response of 15% (data not shown).

322 The shape of the light response curve also determines the transition point from RuBP- to Rubisco-limited  
323 photosynthesis. We explored this effect by investigating the effect of varying the convexity,  $\theta_j$ , which is  
324 assumed to be the same as the convexity of overall photosynthesis. At EucFACE, this parameter is we estimated  
325 to this parameter be as 0.48 based on data from light-response curves of photosynthesis collected on site,  
326 indicating a shallow curvature and a high light saturation points, in contrast to the more commonly assumed  
327 0.85, representing a steeper curvature and a lower light saturation point. Using a value of 0.85 for  $\theta_j$  resulted in a  
328 much lower PAR required for photosynthesis to become Rubisco limited (dashed curves in Figure 7). With a  $\theta_j$   
329 of 0.85 and a J:V ratio of 1.7, MAESPA estimated 40% of photosynthesis to be RuBP-regeneration limited  
330 under ambient conditions and a direct GPP response of 16% (data not shown). With a  $\theta_j$  of 0.85 and a J:V ratio  
331 of 2, MAESPA estimated just 34% of photosynthesis to be RuBP-regeneration limited under ambient conditions  
332 and a direct GPP response of 18% (Figure S2). The simulated CO<sub>2</sub> response of canopy carbon uptake thus  
333 depends heavily on the parameterisation of light response and J:V ratio.

334

### 335 3.2 Acclimation of photosynthesis

336 The above calculations are made considering only the instantaneous response of photosynthesis to  $eC_a$ .  
337 However, photosynthetic acclimation was observed at leaf scale (Ellsworth et al., in prep), and will also reduce  
338 the response of GPP to  $eC_a$  at the canopy scale. At the leaf-level, photosynthesis measured in the elevated rings  
339 after five years of treatment ( $A_{long}$ ) was 19% higher than that measured in ambient rings (Figure 4e; Ellsworth et  
340 al. 2017).  $A_{long}$  thus accounts for the photosynthetic acclimation in the elevated rings after four years of exposure  
341 to  $eC_a$ .  $A_{long}$  is considerably smaller than  $A_{inst}$  (19% vs. 33%; Figure 4 a and e), indicating a large effect of  
342 photosynthetic acclimation on the  $eC_a$  response of light-saturated photosynthesis.

343 Accounting for the impact of photosynthetic acclimation in MAESPA, by using the  $V_{cmax}$  from elevated rings  
344 (“field” vs. “ambient” scenarios) reduced the response of GPP to  $C_a$  from 11% to 10% ( $GPP_{long}$ ; Figure 4f). As  
345 such, the photosynthetic acclimation had a relatively modest impact on the modelled annual GPP in the model.  
346 The small impact of photosynthetic acclimation on canopy photosynthesis relative to the effect on leaf  
347 photosynthesis can be explained by the fact that the leaf photosynthesis data are measured under saturating light  
348 and thus are typically Rubisco-limited, so a reduction in  $V_{cmax}$  had a large effect. In contrast, at the canopy scale,  
349 much of the photosynthesis was limited by RuBP-regeneration and was largely unaffected by a reduction in  
350  $V_{cmax}$ .

### 351 3.3 Influence of LAI

352 The realised GPP response to  $eC_a$  also depends on the canopy structure, specifically the LAI. In this experiment,  
353 there was no significant change in LAI with  $eC_a$  (-4% ± 5%; Figure 4g; see also Duursma et al. 2016). The  
354 effect of  $eC_a$  on LAI was calculated as the average effect between elevated and ambient annual mean LAI.  
355 However, there was inherent variability in LAI across the rings (Figure 2a), which does not fundamentally

356 change the effect of  $eC_a$  but requires a detailed analysis of the potential effects of natural variability on the  
357 response to  $eC_a$ .

358

359 The small pre-treatment difference in LAI across rings gives rise to a range of estimates for the GPP response to  
360  $eC_a$  in the field ( $6\% \pm 8\%$ ; Figure 4h). This result is explored further in Figure 8, which combines the results  
361 from “ambient”, “elevated”, and “field” scenarios. The average GPP across all six rings under ambient  $C_a$  was  
362  $1574 \text{ g C m}^{-2} \text{ yr}^{-1}$  over the four-year simulation (“ambient scenario”; Figure 8). However, there was significant  
363 variability in ambient GPP across rings, related in part to the inherent variability in LAI across rings. We  
364 characterised the pre-existing differences in LAI by the initial LAI ( $LAI_i$ ), measured on 26 October 2012. These  
365 initial values are low, because they are measured immediately before the seasonal leaf flush, but characterise the  
366 difference in LAI across rings over the full experimental period. Rings 1 and 4 (both experimental rings) have  
367 the lowest  $LAI_i$  ( $<0.3 \text{ m}^2 \text{ m}^{-2}$ ) and thus the lowest average GPP under ambient conditions ( $1206 \text{ g C m}^{-2} \text{ yr}^{-1}$ ).  
368 Ring 5 (the other experimental ring) has the second highest  $LAI_i$  ( $\sim 0.4 \text{ m}^2 \text{ m}^{-2}$ ) and also the highest GPP under  
369 ambient conditions ( $2359 \text{ g C m}^{-2} \text{ yr}^{-1}$ ). The variability among rings in ambient GPP ( $SD = 15\%$ ) is thus larger  
370 than the modelled direct effect of  $C_a$  on GPP, which is similar in all rings ( $+11\%$ ).

371 Owing to the variability among rings represented by  $LAI_i$ , the estimated mean GPP response to  $eC_a$  across the  
372 experimental rings has a sizeable confidence interval ( $\pm 8\%$ , Figure 4h). The actual  $eC_a$  response was estimated  
373 as an average effect between the ambient and elevated GPP values considering the impacts of photosynthetic  
374 acclimation and inter-ring variability. The average GPP of experimental rings under field conditions ( $eC_a$ ) was  
375 estimated to be  $1698 \text{ g C m}^{-2} \text{ yr}^{-1}$  while the average GPP of control rings under field conditions (ambient  $C_a$ )  
376 was  $1599 \text{ g C m}^{-2} \text{ yr}^{-1}$ , an increase of  $6\%$  as shown in the Figure 4h. The variation of annual average GPP of the  
377 control and experimental groups (blue and red squares in Figure 8) are thus represented by the CI in Figure 4h.

378

#### 379 4. Discussion

380 We have showed how a large response of leaf-level photosynthesis to  $eC_a$  diminishes when integrated to the  
381 canopy-scale, according to the synthesis of four years of leaf measurements at EucFACE with the stand-scale  
382 model, MAESPA. We estimated that the canopy GPP of a mature *Eucalyptus* woodland under ambient  $C_a$   
383 conditions varied from  $1084\text{--}2129 \text{ g C m}^{-2} \text{ yr}^{-1}$  by ring and year with a mean of  $1574 \text{ g C m}^{-2} \text{ yr}^{-1}$ . The model,  
384 constrained by site measurements, predicted that once scaled to the canopy, the response of GPP to  $eC_a$  only  
385 increased by  $6\%$  ( $95\% \text{ CI of } \pm 8\%$ ) compared to the  $19\%$  ( $95\% \text{ CI of } \pm 5\%$ ) observed in leaf-scale measurements.  
386 We were able to quantify the response of GPP to  $eC_a$  and attribute the reduction in the response to various  
387 factors including: (i) Rubisco versus RuBP-regeneration limitations to photosynthesis; (ii) photosynthetic  
388 acclimation; (iii) inter-ring variability in LAI. Together these findings provide valuable insights into the relative  
389 importance of each factor and help close a key knowledge gap in our understanding of how mature forests  
390 respond to  $eC_a$ .



#### 391 4.1 Performance of MAESPA under ambient conditions

392 The ambient GPP of EucFACE estimated by MAESPA was comparable to that measured with eddy covariance  
393 in similar evergreen Eucalypt forests in Southeast Australia. In a nearby eddy covariance site (<1 km), ,  
394 Renchon et al. (2018) estimated the ecosystem GPP from eddy covariance to be 1561 g C m<sup>-2</sup> yr<sup>-1</sup> during 2013  
395 to 2016 which is within the range estimated for the ambient rings in this study, though this latter site and the  
396 EucFACE are not the same in terms of canopy structure and LAI. Furthermore, our version of MAESPA was  
397 evaluated against leaf photosynthesis and whole-tree sap flow measurements in EucFACE (R<sup>2</sup> of 0.77 and 0.8,  
398 respectively; Yang et al., [in review 2019](#)). These comparisons indicate MAESPA is a useful tool to explore the  
399 canopy carbon uptake and the predicted GPP could provide a baseline to future studies.

#### 400 4.2 RuBP-regeneration limited photosynthesis

401 Our results show that the canopy GPP at EucFACE was predominantly limited by RuBP regeneration. The  
402 reason for the frequent RuBP-regeneration limitation is that the measured J:V ratio was relatively small in  
403 EucFACE (1.7), and stomata tend to close at midday when light levels are higher and Rubisco-limitation is  
404 expected (Gimeno et al., [2016 2015](#)). A lower J:V ratio increases the PAR threshold required for the  
405 photosynthesis model to switch between the RuBP-regeneration limitation and the Rubisco limitation (from  
406 <1000 to <1800 μmol m<sup>-2</sup> s<sup>-1</sup>; Figure 7). Previous studies have highlighted the need to consider J:V ratio for a  
407 correct prediction of CO<sub>2</sub> response (Long et al, 2004; Zaehle et al., 2014; Rogers et al., 2017). However, as  
408 shown by Zaehle et al. (2014), Medlyn et al. (2015), and Rogers et al. (2017), current models differ in their  
409 predictions of the transition from RuBP-regeneration- to Rubisco-limited photosynthesis, suggesting the  
410 uncertainty of predicted CO<sub>2</sub> response of GPP could be reduced by using a realistic J:V ratio.

411 Previous modelling studies applying MAESPA to eC<sub>a</sub> experiments both assumed higher J:V ratio (2) and  
412 estimated higher GPP response to eC<sub>a</sub> presumably due to less frequent RuBP-regeneration limitation (Wang et  
413 al., 1998; Luo et al., 2001). A J:V ratio of 2 was suggested by Wullschleger (1993) and has been used in many  
414 modelling studies (e.g., the seven terrestrial biosphere models assessed by Rogers et al. (2017) all assumed a J:V  
415 ratio of 1.9-2). Global terrestrial biosphere models such as JULES and others frequently estimate J<sub>max</sub> on the  
416 basis of this ratio (e.g., Clark et al. 2011). However, the relatively low J:V ratio observed at EucFACE is not  
417 unique. ~~In At~~ the Duke Forest FACE site in the US, Ellsworth et al. (2012) reported a J:V ratio of ~1.7 which is  
418 the same as that estimated for EucFACE. Kattge and Knorr (2007) analysed V<sub>max</sub> and J<sub>max</sub> values from 36  
419 species across the world and found a low J:V ratio (<1.8) in herbaceous, coniferous, and broadleaved species.  
420 Most recently, Kumarathunge et al. (2018) studied the variation in J:V ratio in datasets obtained from around the  
421 globe and found ~~a consistent relationship with that it declined with increasing~~ growing season temperature. The  
422 ratio varied from 2.5 in tundra environments to < 1.5 in tropical environments. The value of 1.7 observed at  
423 EucFACE falls within this prediction for the prevailing growth temperature at this site. The inclusion of this  
424 relationship between ~~this relationship~~ of J:V ratio and temperature will thus be important for capturing the GPP  
425 response to eC<sub>a</sub> globally.

426 We also found that the ~~curvature convexity~~ of the light response of photosynthesis affected the predicted GPP  
427 response to eC<sub>a</sub> (Figure 7). The parameter value we fitted to data measured *in situ* ( $\theta_1 = 0.48$ ) is lower than the  
428 value commonly assumed in the models (e.g., 0.7 in Bonan et al., 2011 typically around 0.85, e.g., 0.9 in  
429 Medlyn et al., 2002; 0.7 in Bonan et al., 2011; 0.85 in Harverd et al., 2018). Note that some model studies

430 *assume that  $\theta_j$  to be lower than the convexity of overall photosynthesis (typically over 0.8; e.g., 0.9 in Medlyn et*  
431 *al., 2002; 0.85 in Haverd et al., 2018). Here we assumed that the convexity of electron transport rate and overall*  
432 *photosynthesis are the same (see Supplementary Text S1 for details). Nonetheless, our relatively low  $\theta_j$  value*  
433 *(<0.7) is not unique, as it is also supported by a number of studies on different species around the world (Ögren,*  
434 *1993; Valladares et al., 1997; Lewis et al., 2000; Hjelm and Ögren, 2004). The inclusion of higher  $\theta_j$  value*  
435 *would predict a much higher direct GPP response to  $eC_a$  (e.g., 16% versus 11% in this study), because higher  $\theta_j$*   
436 *results in a large proportion of GPP being Rubisco-limited. This finding calls for careful examination of the*  
437 *light-response of photosynthesis, which has a large effect on the predicted  $eC_a$  response*

#### 438 **4.2 Photosynthetic acclimation**

439 Some degree of photosynthetic acclimation (i.e., a long-term reduction of  $V_{\text{cmax}}$  under  $eC_a$ ) has been widely  
440 reported in FACE studies and has been attributed to a reduction of leaf nitrogen concentration (Saxe et al., 1998;  
441 Ainsworth and Long, 2005). The response of GPP to  $eC_a$  would be linearly related to  $V_{\text{cmax}}$  if photosynthesis  
442 were mostly limited by Rubisco activity. Photosynthetic acclimation was responsible for the reduced response of  
443 leaf-scale light-saturated photosynthesis from 33% ( $A_{\text{inst}}$ ) to 19% ( $A_{\text{long}}$ ). However, this reduction in  $V_{\text{cmax}}$   
444 translated into only a ~2% reduction in GPP modelled by MAESPA. Wang et al. (1998) also showed that  
445 photosynthetic acclimation (-21% in  $V_{\text{cmax}}$ ) reduced modelled canopy GPP by only 6% due to RuBP-  
446 regeneration being the primary limitation of canopy photosynthesis. These findings thus suggest that  
447 photosynthetic acclimation may only have a small effect in the GPP response to  $eC_a$  when canopy  
448 photosynthesis is mostly RuBP-regeneration limited. This response is thus consistent with the hypothesis that  
449 the reduction in  $V_{\text{cmax}}$  represents a re-allocation of nitrogen to optimise nitrogen use efficiency under  $eC_a$  (Chen  
450 et al., 1993; Medlyn et al., 1996).

#### 451 **4.3 Constraining the carbon balance response to $eC_a$**

452 At EucFACE, after four years of  $eC_a$  treatment, there was no evidence of increased above-ground tree growth  
453 (Ellsworth et al., 2017). Nor have the trees at EucFACE shown any significant change in LAI (Duursma et al.,  
454 2016). The relatively small response of GPP and the effect of ring-to-ring variation provides important context  
455 for these statistically non-significant responses of tree growth at the stand scale at EucFACE. Firstly, the effect  
456 size calculated for GPP of +11% (+ 169 g C m<sup>-2</sup> yr<sup>-1</sup>) constrains the likely effect size for plant growth and other  
457 components of the ecosystem carbon balance and is a more useful baseline for comparison than the response of  
458 light-saturated leaf photosynthesis (+19% = 299 g C).

459 Secondly, the inherent ring-to-ring variation in this natural forest stand is ~~even higher~~ larger than the GPP  
460 response, which highlights the importance of considering both the effect size and ~~uncertainty~~ variability in the  
461 observations than to focus on statistical significance. It is important to note that the EucFACE site could be  
462 considered relatively homogeneous for a mature woodland. The site is flat, trees appear similar-aged, and almost  
463 all the overstory belongs to a single species. In addition, plots were carefully sited to minimise variation in basal  
464 area. However, there are small-scale variations in soil type, depth, and nutrient availability that cause variation  
465 in LAI. This scale of variation is likely to present in other natural forests, and indeed, other studies on mature  
466 trees also note that background variability can contribute to the lack of statistically significant findings (Fatichi  
467 and Leuzinger, 2013; Sigurdsson et al. 2013). We highlight the need to focus on effect size and its uncertainty,

Formatted: Font: Italic

468 rather than the dichotomous significant/non-significant approach when evaluating experimental results from  
469 native forests.

#### 470 **4.4 Implications for terrestrial biosphere models**

471 Seven Terrestrial Biosphere Models (TBMs) were used to predict GPP and LAI responses to  $eC_a$  in advance of  
472 the EucFACE experiment (Medlyn et al. 2016). The predicted  $eC_a$  responses of GPP ranged from +2 to +24%  
473 across the seven models, while the predicted responses of LAI ranged from +1 to +20%. With our results, it is  
474 possible to falsify some of the assumptions made in these model simulations and identify directions for model  
475 improvement. The model with the lowest GPP response (CLM4-P) assumed very strong down-regulation of  
476 photosynthesis owing to phosphorus limitation. However, this down-regulation was not observed here. The  
477 models with the highest GPP responses (GDAY, O-CN, SDGVM) had a J:V ratio of 2 which is higher than that  
478 observed at EucFACE, and also had a positive feedback to GPP via increased LAI (+5-15%), which did not  
479 occur (Duursma et al., 2016). The model rendering most similar prediction for the GPP response to  $eC_a$  to the  
480 output of MAESPA incorporating empirical observations was the CABLE model. This latter model predicted an  
481  $eC_a$  response of GPP of ~12% with a large proportion of RuBP-regeneration limited photosynthesis, both of  
482 which are similar to the findings in this study. Future TBMs may benefit from incorporating a more realistic  
483 representation of the relative contribution of RuBP-regeneration- to Rubisco- limited photosynthesis to GPP.  
484 For instance, adding the temperature dependency of J:V ratio could help capture the variation of J:V ratio  
485 globally (e.g., Kumarathunge et al., 2018).

486 Our study provides a number of process-based insights that can be used to improve model performance both  
487 qualitatively and quantitatively. Our modelling exercise is also a major contribution to the understanding of the  
488 EucFACE experiment by quantifying the amount of extra carbon input into the system by canopy-level  
489 photosynthesis and thus providing a reference for assessing the impacts of  $eC_a$  on growth and soil respiration.  
490 Finally, our study highlights that the  $eC_a$  effect on canopy-scale GPP may be considerably lower than the effect  
491 on photosynthesis of the light-saturated leaves, due to contrasting relative limitations to photosynthesis  
492 operating and different scales. In future work, our GPP estimates will be used as an input to calculate the overall  
493 effect of  $eC_a$  on the carbon balance at the whole EucFACE site.

#### 494 **Acknowledgements**

495 JY was supported by a PhD scholarship from Hawkesbury Institute for the Environment, Western Sydney  
496 University. MGDK was supported by NSW Research Attraction and Acceleration Program (RAAP).

497 EucFACE was built as an initiative of the Australian Government as part of the Nation-building Economic  
498 Stimulus Package and is supported by the Australian Commonwealth in collaboration with Western Sydney  
499 University. It is also part of a TERN Super-site facility.

500 We thank Vinod Kumar, Craig McNamara and Craig Barton, for their excellent technical support. We also  
501 thank Elise Dando for help in measuring crown radius, Steven Wohl for crane driving, Julia Cooke and Burhan  
502 Amiji for installing the neutron probe access tubes.

#### 503 **Author contribution statement**

504 JY, BM, MDK, and RD conceived and designed the analysis. KC, DE, and TG designed sampling of leaf  
505 physiological data, while DE and RD designed sampling of canopy structure data. KC, DE, TG, AWK, RD and  
506 JY collected data. RD and DK provided analysis tools. JY and BM performed the analysis. JY, BM, MDK, and  
507 MJ wrote the paper. All authors edited and approved the manuscript.

508

509

## 510 References

511 Ainsworth, E. A. and Long, S. P.: What have we learned from 15 years of free-air CO<sub>2</sub> enrichment (FACE)? A  
512 meta-analytic review of the responses of photosynthesis, canopy properties and plant production to rising CO<sub>2</sub>,  
513 *New Phytol.*, 165(2), 351–372, doi:10.1111/j.1469-8137.2004.01224.x, 2005.

514 Bernacchi, C. J., Singaas, E. L., Pimentel, C., Portis Jr, A. R. and Long, S. P.: Improved temperature response  
515 functions for models of Rubisco-limited photosynthesis, *Plant, Cell Environ.*, 24(2), 253–259,  
516 doi:10.1046/j.1365-3040.2001.00668.x, 2001.

517 Bonan, G. B. and Doney, S. C.: Climate, ecosystems, and planetary futures: The challenge to predict life in  
518 Earth system models, *Science* (80-), 359(6375), doi:10.1126/science.aam8328, 2018.

519 [Bonan, G. B., Lawrence, P. J., Oleson, K. W., Levis, S., Jung, M., Reichstein, M., Lawrence, D. M. and](#)  
520 [Swenson, S. C.: Improving canopy processes in the Community Land Model version 4 \(CLM4\) using global](#)  
521 [flux fields empirically inferred from FLUXNET data. \*J. Geophys. Res.\*, 116\(G2\), 1–22,](#)  
522 [doi:10.1029/2010jg001593, 2011.](#)

523 Chen, J. L., Reynolds, J. F., Harley, P. C. and Tenhunen, J. D.: Coordination theory of leaf nitrogen distribution  
524 in a canopy, *Oecologia*, 93(1), 63–69, doi:10.1007/BF00321192, 1993.

525 Clark, D. B., Mercado, L. M., Sitch, S., Jones, C. D., Gedney, N., Best, M. J., Pryor, M., Rooney, G. G., Essery,  
526 R. L. H., Blyth, E., Boucher, O., Harding, R. J., Huntingford, C. and Cox, P. M.: The Joint UK Land  
527 Environment Simulator (JULES), model description – Part 2: Carbon fluxes and vegetation dynamics, *Geosci.*  
528 *Model Dev.*, 4(3), 701–722, doi:10.5194/gmd-4-701-2011, 2011.

529 Curtis, P. S., and X. Wang (1998), A meta-analysis of elevated CO<sub>2</sub> effects on woody plant mass, form, and  
530 physiology, *Oecologia*, 113(3), 299–313, doi:10.1007/s004420050381.

531 Dawes, M. A., Hättenschwiler, S., Bebi, P., Hagedorn, F., Handa, I. T., Körner, C. and Rixen, C.: Species -  
532 specific tree growth responses to 9 years of CO<sub>2</sub> enrichment at the alpine treeline, *J. Ecol.*, 99(2), 383–394,  
533 doi:10.1111/j.1365-2745.2010.01764.x, 2011.

534 De Kauwe, M. G., Medlyn, B. E., Zaehle, S., Walker, A. P., Dietze, M. C., Wang, Y. P., Luo, Y., Jain, A. K.,  
535 El-Masri, B., Hickler, T., Wårlind, D., Weng, E., Parton, W. J., Thornton, P. E., Wang, S., Prentice, I. C., Asao,  
536 S., Smith, B., Mccarthy, H. R., Iversen, C. M., Hanson, P. J., Warren, J. M., Oren, R. and Norby, R. J.: Where  
537 does the carbon go? A model-data intercomparison of vegetation carbon allocation and turnover processes at  
538 two temperate forest free-air CO<sub>2</sub> enrichment sites, *New Phytol.*, 203(3), 883–899, doi:10.1111/nph.12847,  
539 2014.

540 Donohue, R. J., Mcvicar, T. R. and Roderick, M. L.: Climate-related trends in Australian vegetation cover as  
541 inferred from satellite observations, 1981–2006, *Glob. Chang. Biol.*, 15(4), 1025–1039, doi:10.1111/j.1365-  
542 2486.2008.01746.x, 2009.

Formatted: Font: Italic

543 Donohue, R. J., Roderick, M. L., McVicar, T. R. and Farquhar, G. D.: Impact of CO<sub>2</sub> fertilization on maximum  
544 foliage cover across the globe's warm, arid environments, *Geophys. Res. Lett.*, 40(12), 3031–3035,  
545 doi:10.1002/grl.50563, 2013.

546 Drake, J. E., Power, S. A., Duursma, R. A., Medlyn, B. E., Aspinwall, M. J., Choat, B., Creek, D., Eamus, D.,  
547 Maier, C., Pfautsch, S., Smith, R. A., Tjoelker, M. G. and Tissue, D. T.: Stomatal and non-stomatal limitations  
548 of photosynthesis for four tree species under drought: A comparison of model formulations, *Agric. For.*  
549 *Meteorol.*, 247, 454–466, doi:10.1016/j.agrformet.2017.08.026, 2017.

550 Duursma, R. A. and Medlyn, B. E.: MAESPA: a model to study interactions between water limitation,  
551 environmental drivers and vegetation function at tree and stand levels, with an example application to [CO<sub>2</sub>] ×  
552 drought interactions, *Geosci. Model Dev.*, 5(4), 919–940, doi:10.5194/gmd-5-919-2012, 2012.

553 Duursma, R. A.: Plantecophys - An R package for analysing and modelling leaf gas exchange data, *PLoS One*,  
554 10(11), 1–13, doi:10.1371/journal.pone.0143346, 2015.

555 Duursma, R. A., Gimeno, T. E., Boer, M. M., Crous, K. Y., Tjoelker, M. G. and Ellsworth, D. S.: Canopy leaf  
556 area of a mature evergreen *Eucalyptus* woodland does not respond to elevated atmospheric [CO<sub>2</sub>] but tracks  
557 water availability, *Glob. Chang. Biol.*, 22(4), 1666–1676, doi:10.1111/gcb.13151, 2016.

558 Eamus, D. and Jarvis, P. G.: The direct effects of increase in the global atmospheric CO<sub>2</sub> concentration on natural  
559 and commercial temperate trees and forests, *Advances in Ecological Research*, vol. 19, pp. 1–55., 1989.

560 Ellsworth, D. S., Thomas, R., Crous, K. Y., Palmroth, S., Ward, E., Maier, C., Delucia, E. and Oren, R.:  
561 Elevated CO<sub>2</sub> affects photosynthetic responses in canopy pine and subcanopy deciduous trees over 10 years: A  
562 synthesis from Duke FACE, *Glob. Chang. Biol.*, 18(1), 223–242, doi:10.1111/j.1365-2486.2011.02505.x, 2012.

563 Ellsworth, D. S., Anderson, I. C., Crous, K. Y., Cooke, J., Drake, J. E., Gherlenda, A. N., Gimeno, T. E.,  
564 Macdonald, C. A., Medlyn, B. E., Powell, J. R., Tjoelker, M. G. and Reich, P. B.: Elevated CO<sub>2</sub> does not  
565 increase eucalypt forest productivity on a low-phosphorus soil, *Nat. Clim. Chang.*, 7(4), 279–282,  
566 doi:10.1038/nclimate3235, 2017.

567 Farquhar, G. D., Caemmerer, S. and Berry, J. A.: A biochemical model of photosynthetic CO<sub>2</sub> assimilation in  
568 leaves of C3 species, *Planta*, 149(1), 78–90, doi:10.1007/BF00386231, 1980.

569 Fatichi, S. and Leuzinger, S.: Reconciling observations with modeling: The fate of water and carbon allocation  
570 in a mature deciduous forest exposed to elevated CO<sub>2</sub>, *Agric. For. Meteorol.*, 174–175, 144–157,  
571 doi:10.1016/j.agrformet.2013.02.005, 2013.

572 [Fatichi, S., Pappas, C., Zscheischler, J. and Leuzinger, S.: Modelling carbon sources and sinks in terrestrial](#)  
573 [vegetation, \*New Phytol.\*, 221\(2\), 652–668, doi:10.1111/nph.15451, 2019.](#)

574 Friend, A.: Modelling canopy CO<sub>2</sub> fluxes: are ‘big-leaf’ simplifications justified?, *Glob. Ecol. Biogeogr.*, 10(6),  
575 603–619, 2001.

576 Gimeno, T. E., Crous, K. Y., Cooke, J., O’Grady, A. P., Ósvaldsson, A., Medlyn, B. E. and Ellsworth, D. S.:  
577 Conserved stomatal behaviour under elevated CO<sub>2</sub> and varying water availability in a mature woodland, *Funct.*  
578 *Ecol.*, 30(5), 700–709, doi:10.1111/1365-2435.12532, 2016.

579 Gimeno, T. E., McVicar, T. R., O’Grady, A. P., Tissue, D. T. and Ellsworth, D. S.: Elevated CO<sub>2</sub> did not affect  
580 the hydrological balance of a mature native *Eucalyptus* woodland, *Glob. Chang. Biol.*, 33(0), 0–2,  
581 doi:10.1111/gcb.14139, 2018.

582 Haverd, V., Smith, B., Nieradzik, L., Briggs, P. R., Woodgate, W., Trudinger, C. M., Canadell, J. G. and Cuntz,  
583 M.: A new version of the CABLE land surface model (Subversion revision r4601) incorporating land use and

Formatted: Font: Italic

584 land cover change, woody vegetation demography, and a novel optimisation-based approach to plant  
585 coordination of photosynthesis, *Geosci. Model Dev.*, 11(7), 2995–3026, doi:10.5194/gmd-11-2995-2018, 2018.

586 Hjelm, U. and Ögren, E.: Photosynthetic responses to short-term and long-term light variation in *Pinus*  
587 *sylvestris* and *Salix dasyclados*, *Trees*, 18(6), 622–629, doi:10.1007/s00468-004-0329-8, 2004.

588 IPCC, 2014: Climate Change 2014: Synthesis Report. Contribution of Working Groups I, II and III to the Fifth  
589 Assessment Report of the Intergovernmental Panel on Climate Change [Core Writing Team, R.K. Pachauri and  
590 L.A. Meyer (eds.)]. *IPCC*, Geneva, Switzerland, 151 pp.

591 Joos, F. and Spahni, R.: Rates of change in natural and anthropogenic radiative forcing over the past 20,000  
592 years, *Proc. Natl. Acad. Sci.*, 105(5), 1425–1430, doi:10.1073/pnas.0707386105, 2008.

593 Knauer, J., Zaehle, S., De Kauwe, M. G., Bahar, N. H. A., Evans, J. R., Medlyn, B. E., Reichstein, M. and  
594 Werner, C.: Effects of mesophyll conductance on vegetation responses to elevated CO<sub>2</sub> concentrations in a land  
595 surface model, *Glob. Chang. Biol.*, (September 2018), 1–19, doi:10.1111/gcb.14604, 2019.

596 Keenan, T. F., Hollinger, D. Y., Bohrer, G., Dragoni, D., Munger, J. W., Schmid, H. P. and Richardson, A. D.:  
597 Increase in forest water-use efficiency as atmospheric carbon dioxide concentrations rise, *Nature*, 499(7458),  
598 324–327, doi:10.1038/nature12291, 2013.

599 Kimball, B. A., Mauney, J. R., Nakayama, F. S. I. and Idso, S. B.: Effects of increasing atmospheric CO<sub>2</sub> on  
600 vegetation, *Vegetatio*, 104/105, 65–75 [online] Available from:  
601 <https://link.springer.com/article/10.1007/BF00048145>, 1993.

602 Klein, T., Bader, M. K. F., Leuzinger, S., Mildner, M., Schleppei, P., Siegwolf, R. T. W. and Körner, C.: Growth  
603 and carbon relations of mature *Picea abies* trees under 5 years of free-air CO<sub>2</sub> enrichment, edited by E. Lines, *J.*  
604 *Ecol.*, 104(6), 1720–1733, doi:10.1111/1365-2745.12621, 2016.

605 Körner, C., Asshoff, R., Bignucolo, O., Hattenschwiler, S., Keel, S. G., Pelaez-Riedl, S., Pepin, S., Siegwolf, R.  
606 T. W. and Zotz, G.: Carbon flux and growth in mature deciduous forest trees exposed to elevated CO<sub>2</sub>, *Science*  
607 (80), 309(5739), 1360–1362, 2005.

608 Kumarathunge, D. P., Medlyn, B. E., Drake, J. E., Tjoelker, M. G., Aspinwall, M. J., Battaglia, M., Cano, F. J.,  
609 Carter, K. R., Cavaleri, M. A., Cernusak, L. A., Chambers, J. Q., Crous, K. Y., De Kauwe, M. G., Dillaway, D.  
610 N., Dreyer, E., Ellsworth, D. S., Ghannoum, O., Han, Q., Hikosaka, K., Jensen, A. M., Kelly, J. W. G., Kruger,  
611 E. L., Mercado, L. M., Onoda, Y., Reich, P. B., Rogers, A., Slot, M., Smith, N. G., Tarvainen, L., Tissue, D. T.,  
612 Togashi, H. F., Tribuzy, E. S., Uddling, J., Vårhammar, A., Wallin, G., Warren, J. M. and Way, D. A.:  
613 Acclimation and adaptation components of the temperature dependence of plant photosynthesis at the global  
614 scale, *New Phytol.*, 222(2), 768–784, doi:10.1111/nph.15668, 2019.

615 Le Quéré, C., Andrew, R. M., Friedlingstein, P., Sitch, S., Pongratz, J., Manning, A. C., Korsbakken, J. I.,  
616 Peters, G. P., Canadell, J. G., Jackson, R. B., Boden, T. A., Tans, P. P., Andrews, O. D., Arora, V. K., Bakker,  
617 D. C. E., Barbero, L., Becker, M., Betts, R. A., Bopp, L., Chevallier, F., Chini, L. P., Ciais, P., Cosca, C. E.,  
618 Cross, J., Currie, K., Gasser, T., Harris, I., Hauck, J., Haverd, V., Houghton, R. A., Hunt, C. W., Hurtt, G.,  
619 Ilyina, T., Jain, A. K., Kato, E., Kautz, M., Keeling, R. F., Klein Goldewijk, K., Körtzinger, A., Landschützer,  
620 P., Lefèvre, N., Lenton, A., Lienert, S., Lima, I., Lombardozi, D., Metzl, N., Millero, F., Monteiro, P. M. S.,  
621 Munro, D. R., Nabel, J. E. M. S., Nakaoka, S., Nojiri, Y., Padín, X. A., Pregon, A., Pfeil, B., Pierrot, D.,  
622 Poulter, B., Rehder, G., Reimer, J., Rödenbeck, C., Schwinger, J., Séférian, R., Skjelvan, I., Stocker, B. D.,  
623 Tian, H., Tilbrook, B., van der Laan-Luijkx, I. T., van der Werf, G. R., van Heuven, S., Viovy, N., Vuichard, N.,  
624 Walker, A. P., Watson, A. J., Wiltshire, A. J., Zaehle, S. and Zhu, D.: Global Carbon Budget 2017, *Earth Syst.*  
625 *Sci. Data Discuss.*, (November), 1–79, doi:10.5194/essd-2017-123, 2017.

626 Lewis, J. D., McKane, R. B., Tingey, D. T. and Beedlow, P. A.: Vertical gradients in photosynthetic light  
627 response within an old-growth Douglas-fir and western hemlock canopy, *Tree Physiol.*, 20(7), 447–456,  
628 doi:10.1093/treephys/20.7.447, 2000.

629 Long, S. P., Ainsworth, E. A., Rogers, A. and Ort, D. R.: Rising atmospheric carbon dioxide: Plants FACE the  
630 Future, *Annu. Rev. Plant Biol.*, 55(1), 591–628, doi:10.1146/annurev.arplant.55.031903.141610, 2004.

631 Luo, Y., Medlyn, B., Hui, D., Ellsworth, D., Reynolds, J. and Katul, G.: Gross primary productivity in duke  
632 forest: Modeling synthesis of CO<sub>2</sub> experiment and eddy-flux data, *Ecol. Appl.*, 11(1), 239–252,  
633 doi:10.2307/3061070, 2001.

634 Medlyn, B. E.: Interactive effects of atmospheric carbon dioxide and leaf nitrogen concentration on canopy light  
635 use efficiency: A modeling analysis, *Tree Physiol.*, 16(1–2), 201–209, doi:10.1093/treephys/16.1-2.201, 1996.

636 Medlyn, B., Badeck, F.-W., De Pury, D., Barton, C., Broadmeadow, M., Ceulemans, R., De Angelis, P.,  
637 Forstreuter, M., Jach, M., Kellomäki, S., Laitat, E., Marek, M., Philippot, S., Rey, A., Strassmeyer, J., Laitinen,  
638 K., Liozon, R., Portier, B., Robertntz, P., Wang, K. and Jarvis, P.: Effects of elevated [CO<sub>2</sub>] on photosynthesis  
639 in European forest species: a meta-analysis of model parameters, *Plant Cell Environ.*, 22, 1475–1495, 1999.

640 Medlyn, B. E., De Kauwe, M. G., Zaehle, S., Walker, A. P., Duursma, R. A., Luus, K., Mishurov, M., Pak, B.,  
641 Smith, B., Wang, Y. P., Yang, X., Crous, K. Y., Drake, J. E., Gimeno, T. E., Macdonald, C. A., Norby, R. J.,  
642 Power, S. A., Tjoelker, M. G. and Ellsworth, D. S.: Using models to guide field experiments: *a priori*  
643 predictions for the CO<sub>2</sub> response of a nutrient- and water-limited native *Eucalypt* woodland, *Glob. Chang. Biol.*,  
644 22(8), 2834–2851, doi:10.1111/gcb.13268, 2016.

645 Medlyn, B. E., Dreyer, E., Ellsworth, D., Forstreuter, M., Harley, P. C., Kirschbaum, M. U. F., Le Roux, X.,  
646 Montpied, P., Strassmeyer, J., Walcroft, a., Wang, K. and Loustau, D.: Temperature response of parameters of  
647 a biochemically based model of photosynthesis. II. A review of experimental data, *Plant, Cell Environ.*, 25(9),  
648 1167–1179, doi:10.1046/j.1365-3040.2002.00891.x, 2002.

649 Medlyn, B. E., Duursma, R. A., Eamus, D., Ellsworth, D. S., Prentice, I. C., Barton, C. V. M., Crous, K. Y., De  
650 Angelis, P., Freeman, M. and Wingate, L.: Reconciling the optimal and empirical approaches to modelling  
651 stomatal conductance, *Glob. Chang. Biol.*, 17(6), 2134–2144, doi:10.1111/j.1365-2486.2010.02375.x, 2011.

652 Medlyn, B. E., Zaehle, S., De Kauwe, M. G., Walker, A. P., Dietze, M. C., Hanson, P. J., Hickler, T., Jain, A.  
653 K., Luo, Y., Parton, W., Prentice, I. C., Thornton, P. E., Wang, S., Wang, Y. P., Weng, E., Iversen, C. M.,  
654 Mccarthy, H. R., Warren, J. M., Oren, R. and Norby, R. J.: Using ecosystem experiments to improve vegetation  
655 models, *Nat. Clim. Chang.*, 5(6), 528–534, doi:10.1038/nclimate2621, 2015.

656 Morison, J. I. L.: Sensitivity of stomata and water use efficiency to high CO<sub>2</sub>, *Plant, Cell Environ.*, 8, 467–474,  
657 1985.Niinemets, Ü., Keenan, T. F. and Hallik, L.: A worldwide analysis of within-canopy variations in leaf  
658 structural, chemical and physiological traits across plant functional types, *New Phytol.*, 205(3), 973–993,  
659 doi:10.1111/nph.13096, 2015.

660 Norby, R. J., DeLucia, E. H., Gielen, B., Calfapietra, C., Giardina, C. P., King, J. S., Ledford, J., McCarthy, H.  
661 R., Moore, D. J. P., Ceulemans, R., De Angelis, P., Finzi, A. C., Karnosky, D. F., Kubiske, M. E., Lukac, M.,  
662 Pregitzer, K. S., Scarascia-Mugnozza, G. E., Schlesinger, W. H. and Oren, R.: Forest response to elevated CO<sub>2</sub>  
663 is conserved across a broad range of productivity, *Proc. Natl. Acad. Sci.*, 102(50), 18052–18056,  
664 doi:10.1073/pnas.0509478102, 2005.

665 Ögren, E.: Convexity of the Photosynthetic Light-Response Curve in Relation to Intensity and Direction of  
666 Light during Growth., *Plant Physiol.*, 101(3), 1013–1019 [online] Available from:  
667 <http://www.ncbi.nlm.nih.gov/pubmed/12231754> <http://www.pubmedcentral.nih.gov/articlerender.fcgi?artid=PMC158720>, 1993.

- 669 Pan, Y., Birdsey, R. A., Fang, J., Houghton, R., Kauppi, P. E., Kurz, W. A., Phillips, O. L., Shvidenko, A.,  
670 Lewis, S. L., Canadell, J. G., Ciais, P., Jackson, R. B., Pacala, S. W., McGuire, A. D., Piao, S., Rautiainen, A.,  
671 Sitch, S. and Hayes, D.: A large and persistent carbon sink in the world's forests, *Science* (80), 333(6045), 988–  
672 993, doi:10.1126/science.1201609, 2011.
- 673 Peñuelas, J., Canadell, J. G. and Ogaya, R.: Increased water-use efficiency during the 20th century did not  
674 translate into enhanced tree growth, *Glob. Ecol. Biogeogr.*, 20(4), 597–608, doi:10.1111/j.1466-  
675 8238.2010.00608.x, 2011.
- 676 [Renchon, A. A., Griebel, A., Metzen, D., Williams, C. A., Medlyn, B., Duursma, R. A., Barton, C. V. M.,  
677 Maier, C., Boer, M. M., Isaac, P., Tissue, D., Resco De Dios, V. and Pendall, E.: Upside-down fluxes Down  
678 Under: CO2net sink in winter and net source in summer in a temperate evergreen broadleaf forest,  
679 \*Biogeosciences\*, 15\(12\), 3703–3716, doi:10.5194/bg-15-3703-2018, 2018.](#)
- 680 Saxe, H., Ellsworth, D. S. and Heath, J.: Tree and forest functioning in an enriched CO<sub>2</sub> atmosphere, *New*  
681 *Phytol.*, 139(3), 395–436, doi:10.1046/j.1469-8137.1998.00221.x, 1998.
- 682 Sigurdsson, B. D., Medhurst, J. L., Wallin, G., Eggertsson, O. and Linder, S.: Growth of mature boreal Norway  
683 spruce was not affected by elevated [CO<sub>2</sub>] and/or air temperature unless nutrient availability was improved, *Tree*  
684 *Physiol.*, 33(11), 1192–1205, doi:10.1093/treephys/tpt043, 2013.
- 685 Silva, L. C. R. and Anand, M.: Probing for the influence of atmospheric CO<sub>2</sub> and climate change on forest  
686 ecosystems across biomes, *Glob. Ecol. Biogeogr.*, 22(1), 83–92, doi:10.1111/j.1466-8238.2012.00783.x, 2013.
- 687 Slevin, D., Tett, S. F. B. and Williams, M.: Multi-site evaluation of the JULES land surface model using global  
688 and local data, *Geosci. Model Dev.*, 8(2), 295–316, doi:10.5194/gmd-8-295-2015, 2015.
- 689 Valladares, F., Allen, M. T. and Pearcy, R. W.: Photosynthetic responses to dynamic light under field conditions  
690 in six tropical rainforest shrubs occurring along a light gradient, *Oecologia*, 111(4), 505–514,  
691 doi:10.1007/s004420050264, 1997.
- 692 van der Sleen, P., Groenendijk, P., Vlam, M., Anten, N. P. R., Boom, A., Bongers, F., Pons, T. L., Terburg, G.  
693 and Zuidema, P. A.: No growth stimulation of tropical trees by 150 years of CO<sub>2</sub> fertilization but water-use  
694 efficiency increased, *Nat. Geosci.*, 8(1), 24–28, doi:10.1038/ngeo2313, 2015.
- 695 Walker, A. P., De Kauwe, M. G., Medlyn, B. E., Zaehle, S., Iversen, C. M., Asao, S., Guenet, B., Harper, A.,  
696 Hickler, T., Hungate, B. A., Jain, A. K., Luo, Y., Lu, X., Lu, M., Luus, K., Megonigal, J. P., Oren, R., Ryan, E.,  
697 Shu, S., Talhelm, A., Wang, Y.-P., Warren, J. M., Werner, C., Xia, J., Yang, B., Zak, D. R. and Norby, R. J.:  
698 Decadal biomass increment in early secondary succession woody ecosystems is increased by CO<sub>2</sub> enrichment,  
699 *Nat. Commun.*, 10(1), 454, doi:10.1038/s41467-019-08348-1, 2019.
- 700 Wang, Y. P., Rey, A. and Jarvis, P. G.: Carbon balance of young birch trees grown in ambient and elevated  
701 atmospheric CO<sub>2</sub> concentrations, *Glob. Chang. Biol.*, 4(8), 797–807, doi:10.1046/j.1365-2486.1998.00170.x,  
702 1998.
- 703 Wujeska-Klaue, A., Crous, K. Y., Ghannoum, O. and Ellsworth, D. S.: Lower photorespiration in elevated CO<sub>2</sub>  
704 reduces leaf N concentrations in mature *Eucalyptus* trees in the field, *Glob. Chang. Biol.*, (August 2018), 1–14,  
705 doi:10.1111/gcb.14555, 2019.
- 706 Wullschlegel, S. D.: Biochemical Limitations to Carbon Assimilation in C<sub>3</sub> Plants—A Retrospective Analysis  
707 of the A/C<sub>i</sub> Curves from 109 Species, *J. Exp. Bot.*, 44(5), 907–920, doi:10.1093/jxb/44.5.907, 1993.
- 708 Yang, J., Medlyn, B. E., De Kauwe, M. G. and Duursma, R. A.: Applying the concept of ecohydrological  
709 equilibrium to predict steady state leaf area index, *J. Adv. Model. Earth Syst.*, 10(8), 1740–1758,  
710 doi:10.1029/2017MS001169, 2018.

Formatted: Font: Italic



711 [Yang J, Duursma RA, De Kauwe MG, Kumarathunge D, Jiang M, Mahmud K, Gimeno TE, Crous KY,](#)  
712 [Ellsworth DS, Peters J, Choat B, Eamus D, Medlyn BE \(2019\) Incorporating non-stomatal limitation improves](#)  
713 [the performance of leaf and canopy models at high vapour pressure deficit. \*Tree Physiol.\*](#)  
714 <https://academic.oup.com/treephys/advance-article/doi/10.1093/treephys/tpz103/5586169>

715 Zaehle, S., Medlyn, B. E., De Kauwe, M. G., Walker, A. P., Dietze, M. C., Hickler, T., Luo, Y., Wang, Y. P.,  
716 El-Masri, B., Thornton, P., Jain, A., Wang, S., Warlind, D., Weng, E., Parton, W., Iversen, C. M., Gallet-  
717 Budynek, A., Mccarthy, H., Finzi, A., Hanson, P. J., Prentice, I. C., Oren, R. and Norby, R. J.: Evaluation of 11  
718 terrestrial carbon-nitrogen cycle models against observations from two temperate Free-Air CO<sub>2</sub> Enrichment  
719 studies, *New Phytol.*, 202(3), 803–822, doi:10.1111/nph.12697, 2014.

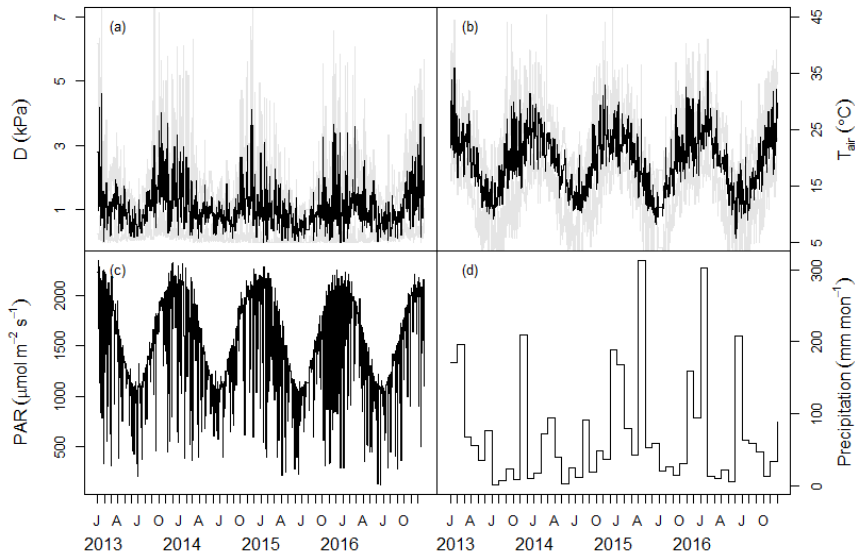
720 Zhu, Z., Piao, S., Myneni, R. B., Huang, M., Zeng, Z., Canadell, J. G., Ciais, P., Sitch, S., Friedlingstein, P.,  
721 Arneeth, A., Liu, R., Mao, J., Pan, Y., Peng, S., Peñuelas, J. and Poulter, B.: Greening of the Earth and its  
722 drivers, *Nat. Clim. Chang.*, 6, early online, doi:10.1038/NCLIMATE3004, 2016.

723

724 **Figures and Captions**

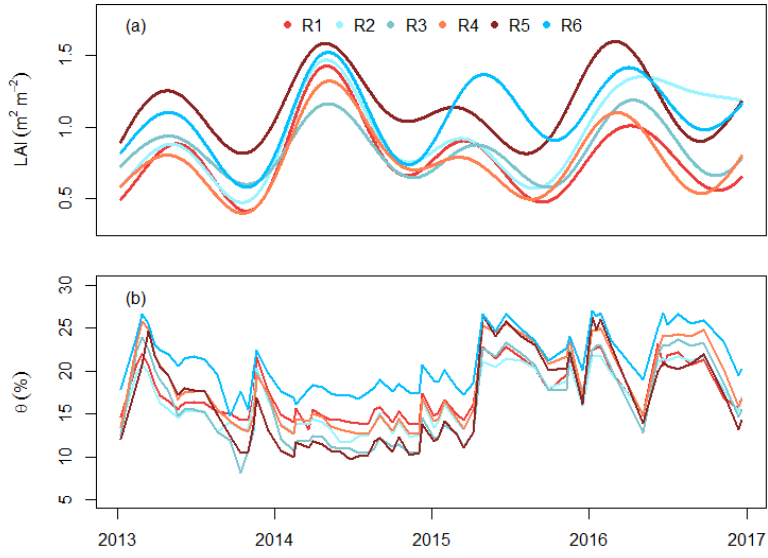
725

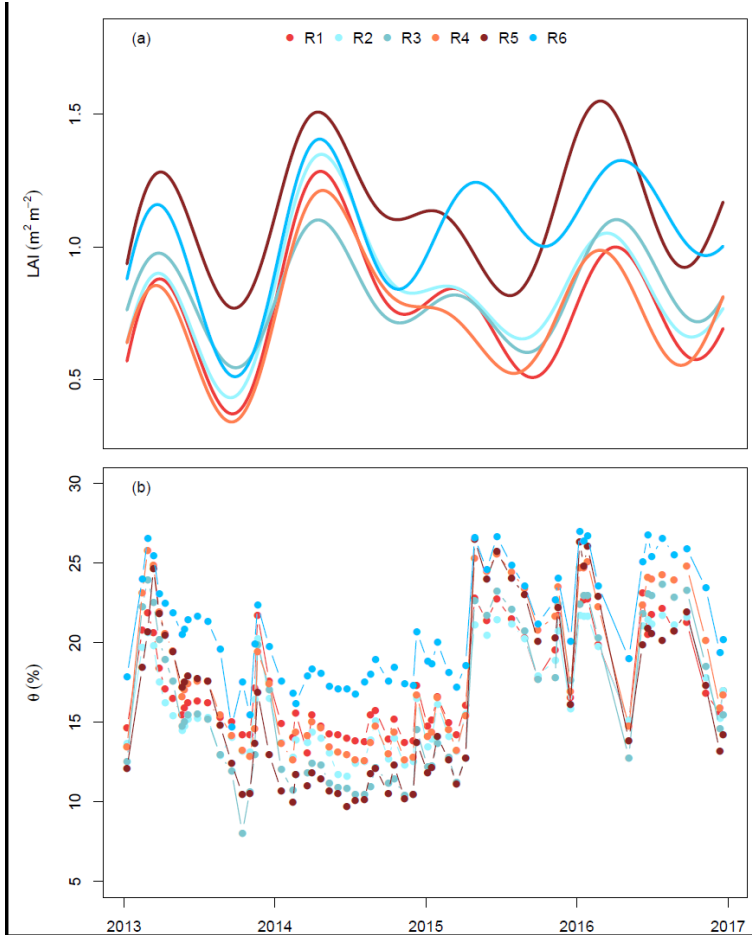
726



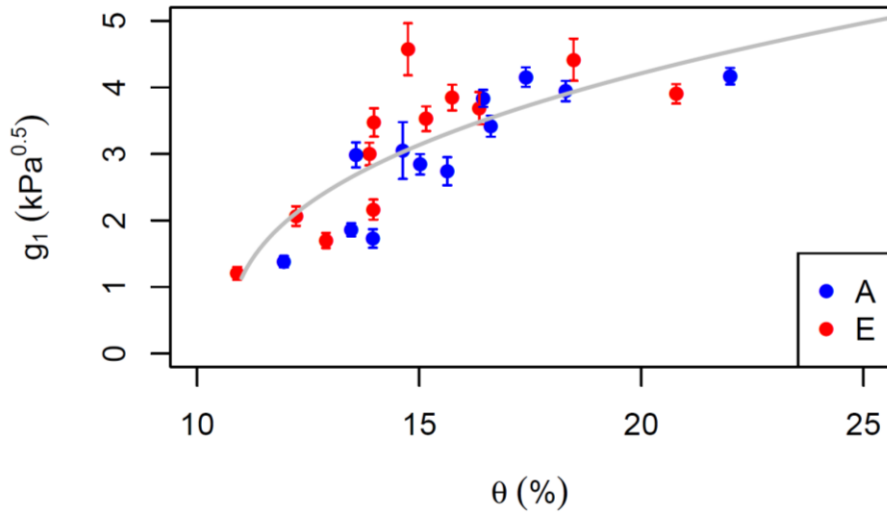
727

728 *Figure 1. Meteorological data measured at the site during the period 2013-2016. Panels show (a) daily mean*  
729 *vapour pressure deficit (D) with shaded area marking the maximum and minimum of the day, (b) daily mean air*  
730 *temperature ( $T_{air}$ ) with shaded area marking the maximum and minimum of the day, (c) daily maximum*  
731 *photosynthetically active radiation (PAR), and (d) monthly total precipitation. Note that precipitation has no*  
732 *direct impact in the model but modifies stomatal conductance via the change in soil moisture.*





734  
 735 Figure 2. (a) Leaf area index (LAI) and (b) soil volumetric water content ( $\theta$ ) used to drive the model. LAI was  
 736 measured-estimated in each ring using the measured-absorbed from measurements of understorey PAR and  
 737 smoothed using a generalized additive model following Duursma et al. (2016).  $\theta$  was measured using neutron  
 738 probes at-in the top 150 cm biweekly and gap-filled using a linear interpolation between two nearest available  
 739 data (Gimeno et al. 2018). Each line colour indicates a different plot. Red colours show elevated  $\text{CO}_2$  plots  
 740 (treatment), while blue colours show ambient  $\text{CO}_2$  plots (control). The x-axis ticks mark the start of each year.

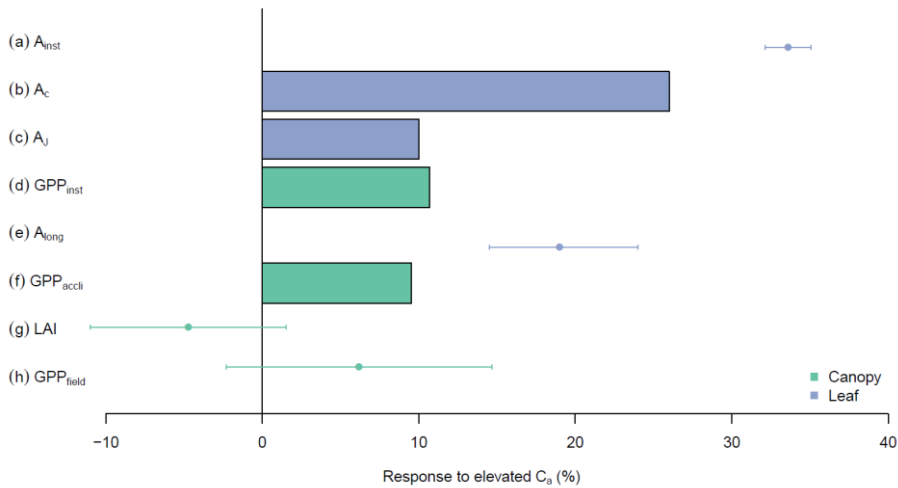


741

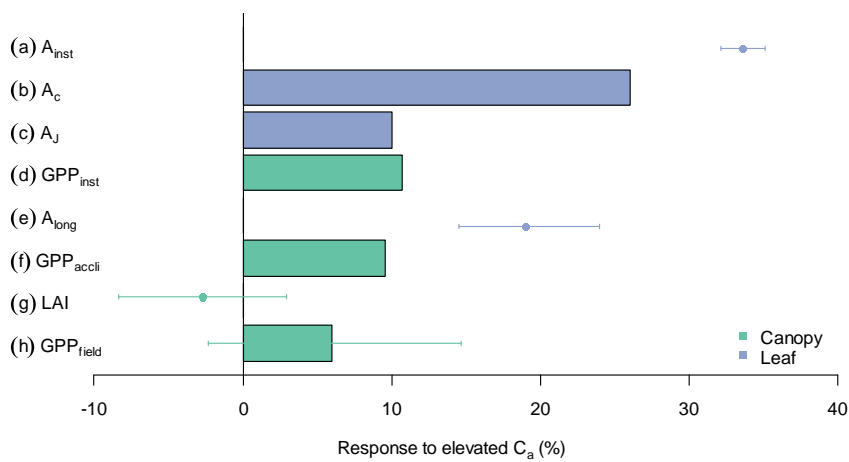
742 Figure 3. The impact of soil moisture content ( $\theta$ ) ~~at~~in the top 150 cm on stomatal regulation.  $g_1$  parameter  
 743 values are fitted to measurements of leaf gas exchange grouped by month and treatment. Red dots are fitted to  
 744 data from elevated rings while blue are ambient rings. ~~The~~Error bars mark indicate the standard errors of the  
 745 fitted values. The grey line shows the fit of Eqn. 2 to the data.

746

747



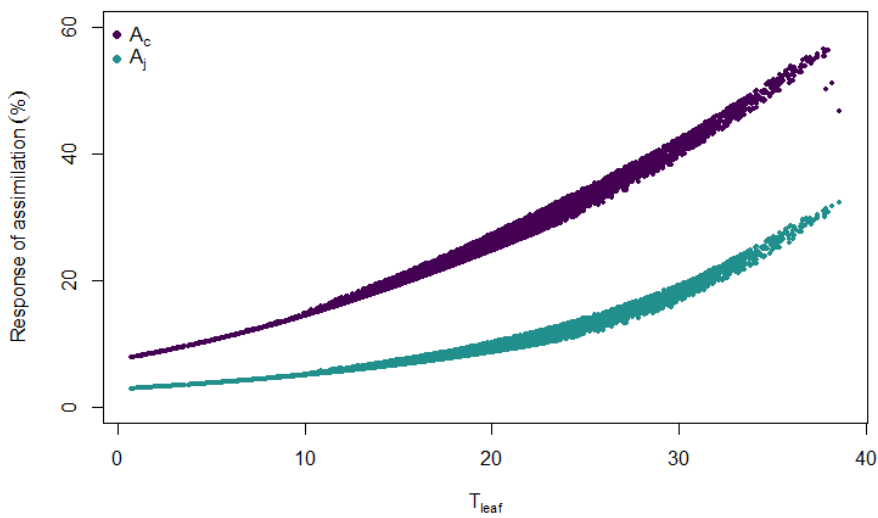
748



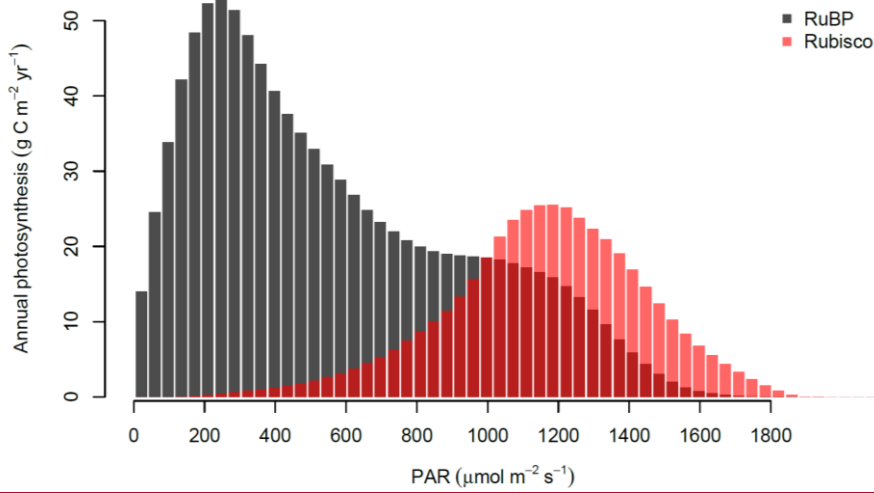
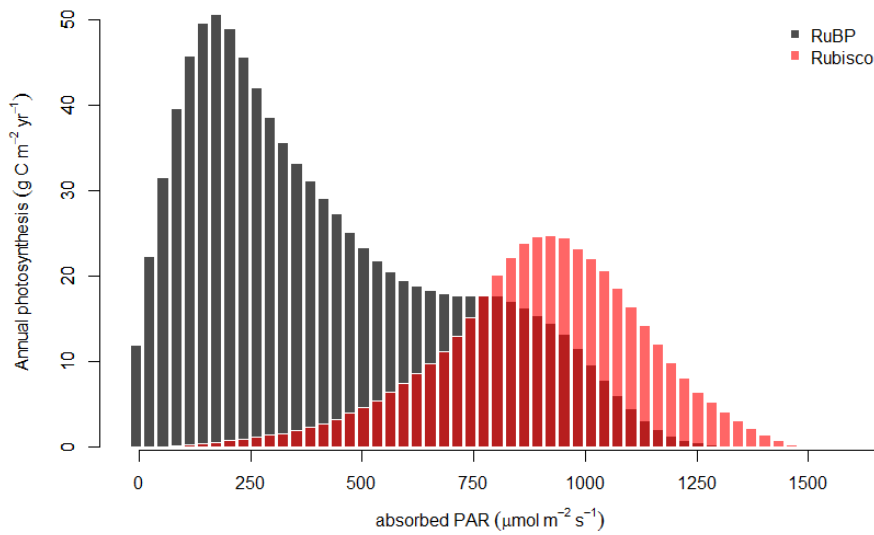
749

750 Figure 4. The response of photosynthesis to  $eC_a$  on different scales and limited by different factors. In summary,  
 751 from top to bottom, the figure demonstrates how a large increase in leaf photosynthesis can diminish into a non-  
 752 statistically significant change in canopy GPP under  $eC_a$ . Entries from top to bottom are as follows. (a)  $A_{inst}$ , the  
 753 instantaneous response of leaf photosynthesis to  $eC_a$  obtained from A-C<sub>1</sub> measurements in ambient rings (error  
 754 bars indicate 95% CI). (b)  $A_c$ , the modelled response of Rubisco-limited leaf photosynthesis, assuming no down-  
 755 regulation, averaged over the range of diurnal air temperatures experienced during the experimental period. (c)  
 756  $A_j$ , the modelled response of RuBP-regeneration limited leaf photosynthesis. (d)  $GPP_{inst}$ , the direct effect of  $eC_a$   
 757 on canopy GPP, modelled with MAESPA, assuming no downregulation of photosynthesis and averaged across  
 758 all six rings. (e)  $A_{long}$ , the long-term response of leaf photosynthesis to  $eC_a$  obtained from leaf photosynthesis  
 759 measured at treatment  $CO_2$  concentrations (see Ellsworth et al. 2017). This value is different from  $A_{inst}$  because

760 it incorporates photosynthetic acclimation. (f)  $GPP_{long}$ , the effect of  $eC_a$  on canopy GPP once the measured  
 761 down-regulation of  $V_{cmax}$  is taken into account. (g) LAI, the measured difference in average LAI between  $eC_a$   
 762 and ambient  $C_a$  rings over the experiment period (data from Duursma et al. 2016). (h)  $GPP_{field}$ , the GPP  
 763 response modelled with MAESPA comparing the three elevated rings with the three ambient rings. The bars  
 764 represent model outputs while points represent observations. See text for further explanation.  
 765



766  
 767 Figure 5. The modelled  $C_a$  response of Rubisco-limited leaf photosynthesis ( $A_c$ ) and RuBP-regeneration-limited  
 768 leaf photosynthesis ( $A_j$ ) against leaf temperature ( $T_{leaf}$ ). The responses are calculated for temperatures during  
 769 the period 2013-2016. Parameters are as given in Table 1, except that  $V_{cmax,25}$  and  $g_1$  were assumed to be  
 770 constant for clarity ( $g_1 = 3.3 \text{ kPa}^{0.5}$  and  $V_{cmax,25} = 90 \text{ } \mu\text{mol m}^{-2} \text{ s}^{-1}$ ).



771

772

773 *Figure 6. Distribution of average annual photosynthesis limited by Rubisco activity and RuBP-regeneration in*  
 774 *bins of absorbed PAR (25-30 μmol m<sup>-2</sup> s<sup>-1</sup>), as calculated by MAESPA across all rings during 2013-2016. The*  
 775 *histogram was constructed by calculating the photosynthesis (either limited by Rubisco or RuBP) falling into*  
 776 *each bin for every half-hour in the “ambient scenario”. These values were then summed to each year and ring*  
 777 *and averaged over six rings and four years.*



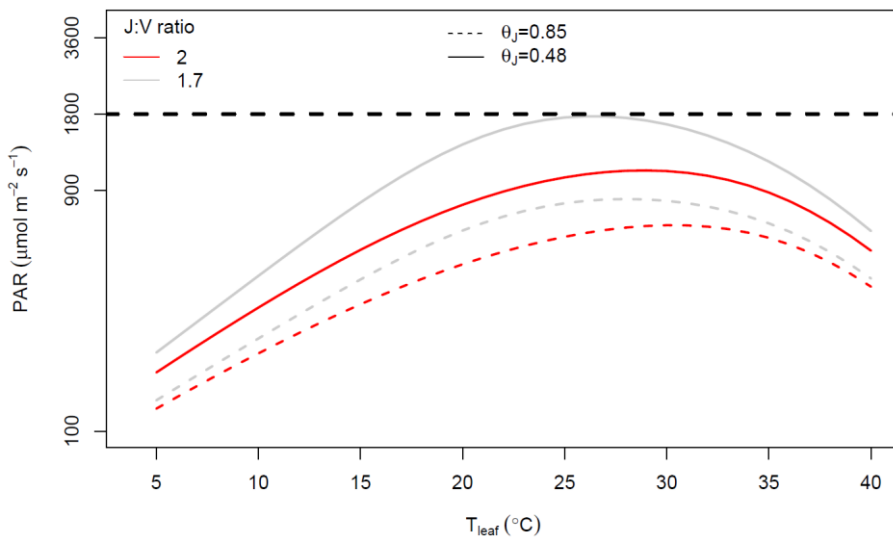
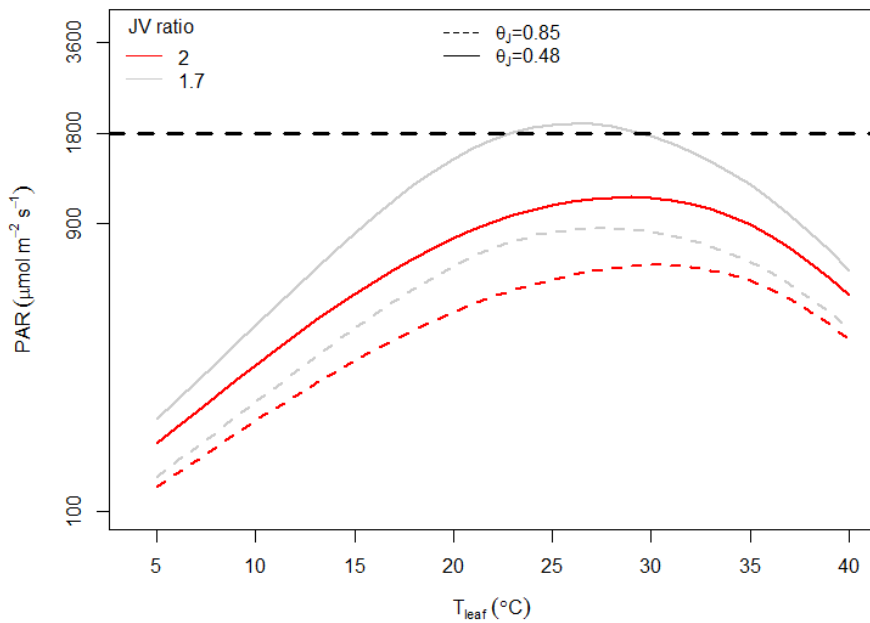
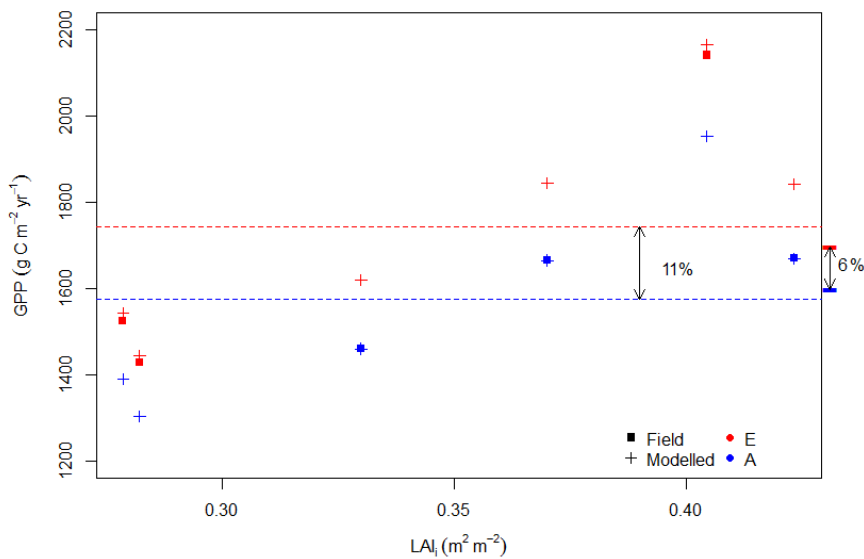


Figure 7. Estimated PAR value at which limitation to photosynthesis shifts from RuBP regeneration to Rubisco at different leaf temperatures and J:V ratios. Rubisco limitation occurs at PAR values above the curves; RuBP regeneration limitation occurs below the curves. The curves were calculated using the Photosyn function in the plantecophys R package (Duursma, 2015). The parameters other than PAR and  $T_{\text{leaf}}$  were assumed to be constant:  $C_a = 390 \mu\text{mol mol}^{-1}$ ;  $D = 1.5 \text{ kPa}$ ;  $g_1 = 3.3 \text{ kPa}^{0.5}$ ;  $V_{\text{max},25} = 90 \mu\text{mol m}^{-2} \text{ s}^{-1}$ . The temperature and

Formatted: Font: Not Italic

Formatted: Font: Not Italic

785 light dependences of photosynthesis were assumed to be the same as in MAESPA. The grey line was predicted  
 786 by assuming  $J_{\max,25} = 153 \mu\text{mol m}^{-2} \text{s}^{-1}$  (i.e., J:V ratio= 1.7). This J:V ratio was observed consistently in  
 787 EucFACE across campaigns and rings. The red line was predicted by assuming  $J_{\max,25} = 180 \mu\text{mol m}^{-2} \text{s}^{-1}$  (i.e.,  
 788 J:V ratio= 2). This J:V ratio was commonly reported and used in other studies. The horizontal dashed line  
 789 shows the PAR =  $1800 \mu\text{mol m}^{-2} \text{s}^{-1}$  at which leaf-level measurements of EucFACE were made. Note the log  
 790 scale of the y axis. The dashed curves are based on quantum yield of electron transport ( $\alpha_j$ ;  $\text{mol mol}^{-1}$ ) and  
 791 convexity of light response of RuBP;  $\theta_j$ ; unitless) values from CABLE model (Haverd et al., 2018). The PAR  
 792 value could be converted to absorbed PAR in Figure 6 with a fraction of 0.8 at our site.



793 Figure 8. The four-year average GPP of all six rings under ambient and  $eC_a$  plotted against initial leaf area  
 794 index (LAI<sub>i</sub>). LAI<sub>i</sub> is the LAI measurement taken on the 26 October 2012 and is a proxy *of* the inherent  
 795 variation among the rings. For all six rings, estimated GPP is shown for ambient  $C_a$  (blue) and  $eC_a$  (red).  
 796 Crosses indicate GPP from simulations by varying  $C_a$  and squares indicate GPP as under field conditions. The  
 797 flat bars on the right hand-side of the plot indicate the average ambient  $C_a$  GPP for ambient rings only (the  
 798 average of blue squares) and average  $eC_a$  GPP for elevated rings only (the average of red squares). Dashed  
 799 lines indicate average ambient  $C_a$  (the average of blue crosses) and  $eC_a$  GPP across all six rings (the average of  
 800 red crosses). The flat bars thus mark the modelled response without inter-ring variability while the dashed lines  
 801 mark the modelled realized response, including inter-ring variability.  
 802

## Supplementary

### TEXT S1. Additional equations of photosynthesis and respiration

$A_{net}$  was modelled as:

$$A_{net} = \min(A_c, A_j) - R_{day} \quad (S1)$$

where  $A_c$  is the gross photosynthetic rate limited by carboxylation rate, while  $A_j$  is the photosynthetic rate limited by electron transport rate;  $R_{day}$  is the light respiration rate in absence of photorespiration ( $\mu\text{mol m}^{-2} \text{s}^{-1}$ ).

$A_c$  is calculated as a function of maximum carboxylation capacity ( $V_{cmax}$ ;  $\mu\text{mol m}^{-2} \text{s}^{-1}$ ) and intercellular  $\text{CO}_2$  concentration ( $C_i$ ):

$$A_c = V_{cmax} \frac{C_i - \Gamma^*}{K_c(1 + \frac{O_i}{K_o}) + C_i} \quad (S2)$$

where  $K_c$  and  $K_o$  are the Michaelis–Menten coefficients of Rubisco activity for  $\text{CO}_2$  and  $\text{O}_2$ , respectively ( $\mu\text{mol mol}^{-1}$  and  $\text{mmol mol}^{-1}$ , respectively), and  $\Gamma^*$  is the  $\text{CO}_2$  compensation point in the absence of mitochondrial respiration ( $\mu\text{mol mol}^{-1}$ );  $O_i$  is intercellular  $\text{O}_2$  concentration ( $\text{mmol mol}^{-1}$ ). The  $K_c$ ,  $K_o$ , and  $\Gamma^*$  are temperature dependent following Bernacchi et al. (2001).

$A_j$  is calculated according to:

$$A_j = \frac{J}{4} \frac{C_i - \Gamma^*}{C_i + 2\Gamma^*} \quad (S3)$$

where  $J$  is the electron transport rate calculated by solving:

$$\theta_j \cdot J^2 - (a_{abs} \cdot \alpha_j \cdot Q_L + J_{max}) \cdot J + a_{abs} \cdot \alpha_j \cdot Q_L \cdot J_{max} = 0 \quad (S4)$$

where  $\theta_j$  describes the curvature electron transport rate (unitless);  $\alpha_j$  is the quantum yield ( $\mu\text{mol } \mu\text{mol}^{-1}$ );  $Q_L$  is the PAR incident on the leaf;  $a_{abs}$  is the absorbance of PAR (1 minus leaf reflectance and transmittance; fraction);  $J_{max}$  is the maximum electron transport rate at the given temperature ( $\mu\text{mol m}^{-2} \text{s}^{-1}$ ). Both  $J_{max}$  and  $V_{cmax}$  depend on leaf temperature and are modelled using a peaked Arrhenius function:

$$k_T = k_{25} \cdot \exp\left(E_a \frac{T_k - 298.15}{298.15 \cdot R_{gas} \cdot T_k}\right) \cdot \left(1 + \frac{\exp(298.15 \cdot \Delta S - H_d)}{298.15 \cdot R_{gas}}\right) / \left(1 + \frac{\exp(T_k \cdot \Delta S - H_d)}{T_k \cdot R_{gas}}\right) \quad (S5)$$

where  $k_T$  is the value of  $J_{max}$  or  $V_{cmax}$  at a given temperature ( $\mu\text{mol m}^{-2} \text{s}^{-1}$ );  $k_{25}$  is the value of  $J_{max}$  or  $V_{cmax}$  at 25 °C;  $\mu\text{mol m}^{-2} \text{s}^{-1}$ );  $T_k$  is the leaf temperature in Kelvin;  $E_a$  is the activation energy which describes the rate of increase of  $k_T$  to temperature ( $\text{J mol}^{-1}$ );  $H_d$  is the deactivation energy which describe the rate of decrease of  $k_T$  to temperature ( $\text{J mol}^{-1}$ );  $\Delta S$  is known as the entropy factor ( $\text{J mol}^{-1} \text{K}^{-1}$ );  $R_{gas}$  is the gas constant ( $\text{J mol}^{-1} \text{K}^{-1}$ ).

The model also assumes  $R_{day}$  to be a fixed fraction (0.7) of  $R_{dark}$  (dark respiration rate;  $\mu\text{mol m}^{-2} \text{s}^{-1}$ ), and uses an Arrhenius temperature response function:

$$R_{dark} = R_{dark.25} \cdot \exp(k_T \cdot (T_{leaf} - 25)) \quad (S6)$$

where  $k_T$  is the sensitivity of  $R_{dark}$  to temperature ( $^{\circ}\text{C}^{-1}$ ); and  $T_{leaf}$  is the leaf temperature ( $^{\circ}\text{C}$ ). MAESPA calculates the leaf temperature that closes the energy balance iteratively (Medlyn et al., 2007).

The light response parameters  $\alpha_j$  and  $\theta_j$  of  $J$  were fitted to light response curves measured *in situ*. We assumed that  $\alpha_j$  is related to quantum yield of photosynthesis ( $\alpha_A$ ):

$$\alpha_j = 4 \cdot \alpha \cdot \frac{C_i + 2\Gamma^*}{C_i - \Gamma^*} \quad (S7)$$

A linear model was fitted to the measured photosynthesis fluxes and absorbed PAR from the initial part of the light response curves ( $< 100 \mu\text{mol m}^{-2} \text{s}^{-1}$ ) and the fitted slope was assumed to be  $\alpha_A$ . This slope was converted to  $\alpha_j$  using Eqn. S7. The curvature of  $J$  ( $\theta_j$ ) was [here](#) assumed to be the same as [that for](#) photosynthesis and thus [could be](#) estimated by fitting the following quadratic relationship:

$$A_{net} = \frac{a_{abs} \cdot \alpha_A \cdot Q_L + A_{max} - \sqrt{(a_{abs} \cdot \alpha_A \cdot Q_L + A_{max})^2 - 4 \cdot a_{abs} \cdot \alpha_A \cdot Q_L \cdot A_{max} \cdot \theta_j}}{2 \cdot \theta_j} + R_{day} \quad (S8)$$

where  $A_{max}$  is the maximum of  $A$ ,  $Q_L$  is the incident PAR and  $a_{abs}$  is the absorptance, which was calculated to be 0.825, by subtracting the fractions of reflectance (0.082) and transmittance (0.093). Eqn. S8 was fitted to the full light response curves using non-linear least squared method to obtain the values of  $A_{max}$  and  $\theta_j$ , assuming  $\alpha_A$  from above. Since the fitting [is](#) not significantly different in the ambient and elevated data, this study used one  $\theta_j$  value fitted to all the data. [The assumptions of the quantum yield and convexity being the same between  \$J\$  and overall photosynthesis are further explored by comparing the photosynthesis predicted by the fitted  \$\alpha\_A\$ ,  \$A\_{max}\$ , and  \$\theta\_j\$  to the measured light response curve. There's good agreement with a root mean square error of  \$2.97 \mu\text{mol m}^{-2} \text{s}^{-1}\$  and a coefficient of correlation of 0.9, suggesting the assumptions are appropriate in our site.](#)

Formatted: Subscript

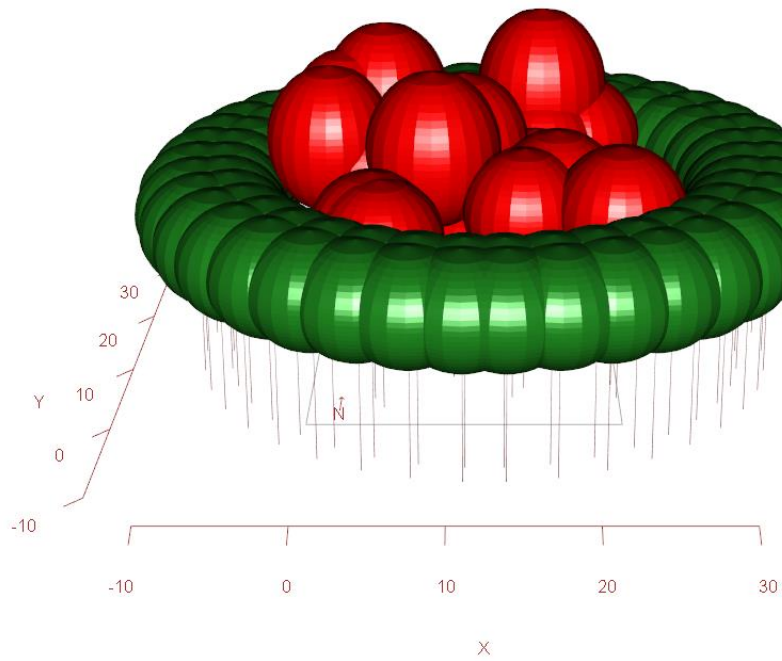


*Figure S1. Example of tree stand as represented in MAESPA. The figure shows the trees in ring 1 (red) and the surrounding trees outside the ring (green). Other rings look similar with realistic tree locations and sizes.*

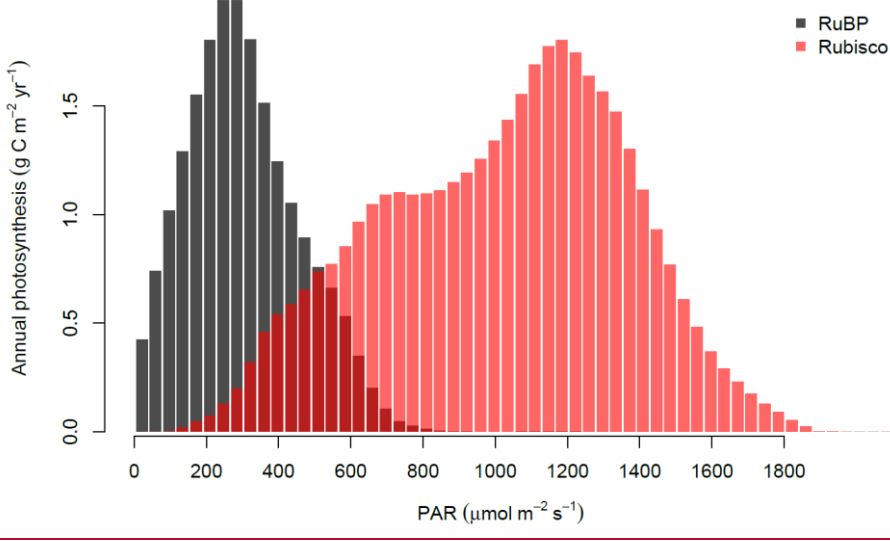
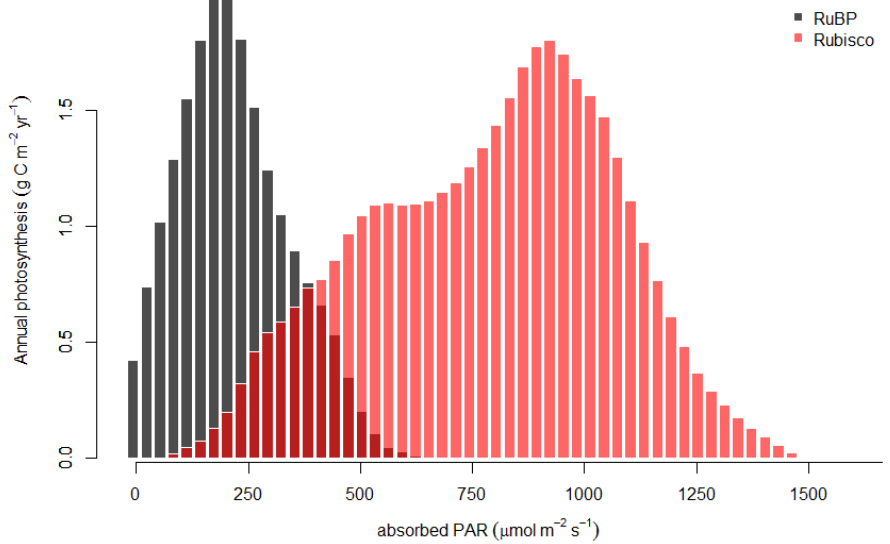


Figure S2. Distribution of average annual photosynthesis limited by Rubisco activity and RuBP-regeneration in bins of *absorbed* PAR ( $25\text{-}30 \mu\text{mol m}^{-2} \text{s}^{-1}$ ), as calculated by MAESPA for all rings during 2013. This figure is produced with a  $\theta_1$  of 0.85 and a J:V ratio of 2, which represents common model assumptions for these values.